Chapter 10: ***Numerical Weather Prediction over Africa*** **– Lead author: Sean Milton**

- Growth of NWP arose from
  - A long tradition of observing the weather,
  - Theoretical foundations laid down in fluid dynamics
  - Development of high speed computers allowing numerical forecasts to be produced in real time
- First Numerical Forecast by hand
  - Carried out by Richardson in the early 20th century
  - Deemed failure as it suffered from large errors
  - Research highlighted need for methods to provide balanced initial states
- First Computerized Numerical Forecast
  - Performed by Charney, Fjortoft and von Neuman in 1950
  - Based on improved understanding of barotropic and baroclinic dynamical systems laid down by Rossby, Charney and Eady
- Rapid improvement in skill of numerical weather forecasts for the extra-tropics From all the operational centres (Fig 10.1)

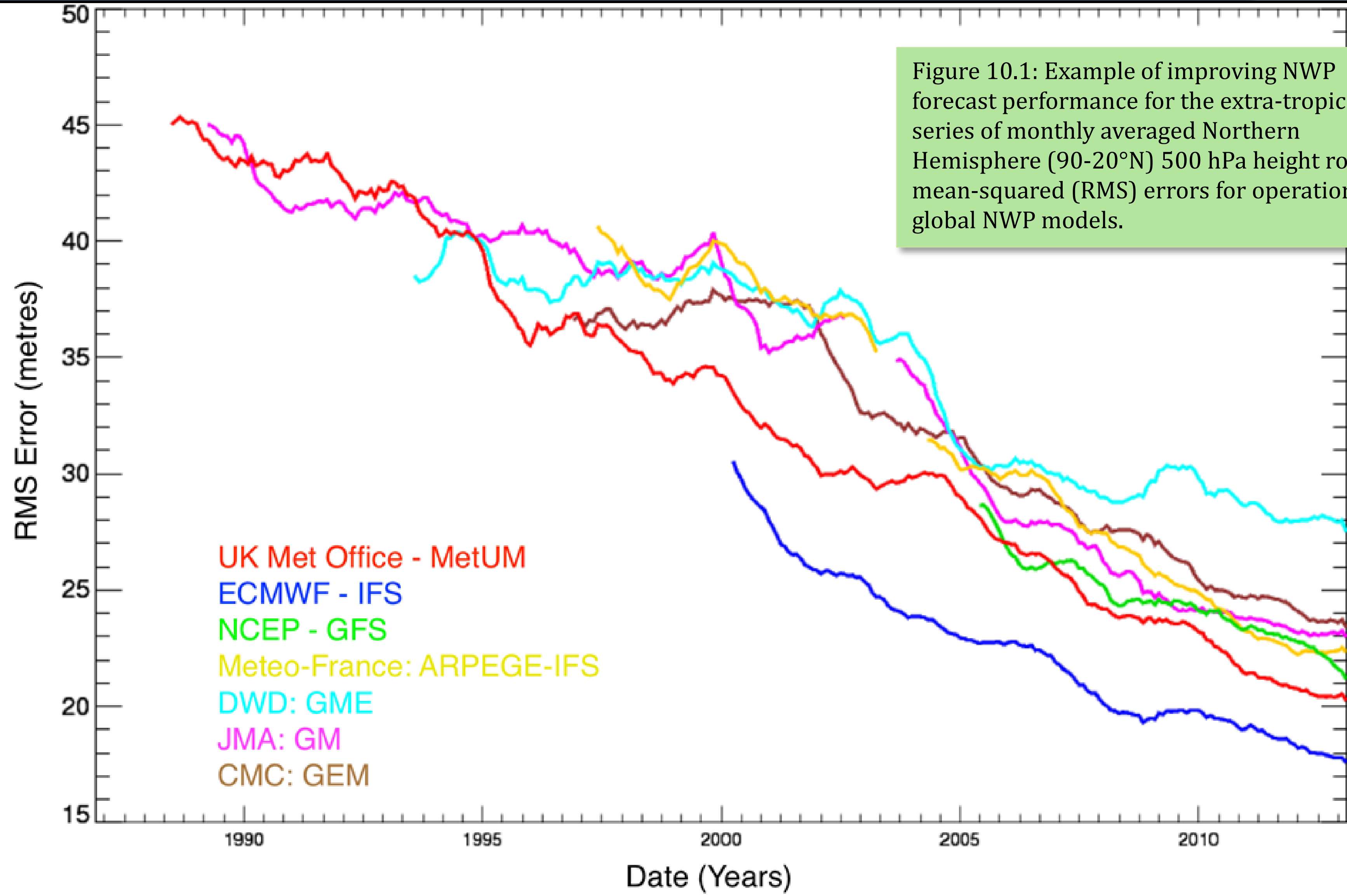

Figure 10.1: Example of improving NWP forecast performance for the extra-tropics. Time series of monthly averaged Northern Hemisphere (90-20°N) 500 hPa height root-mean-squared (RMS) errors for operational global NWP models.

Chapter 10: *Numerical Weather Prediction over Africa* – Lead author: Sean Milton

Factors that contributed to improvement of skill in NWP for the extra-tropics include:
- Deployment of more observing systems (e.g. satellites)
- Improved Data Assimilation
- Improved model resolution
- Continuing physical and dynamical development

Africa and tropics
- Improvements in predicting the large-scale flow over Africa and other tropical regions (Fig 10.2)
- NWP in Africa is still a forecasting challenge – need to incorporate weather and climate regimes

Synoptic Scale Systems
- African Easterly Jet (AEJ)
- African Easterly Wave (AEW)
- Tropical cyclones are linked to tropical cyclogenesis in tropical Atlantic

Key difference to mid-latitude
- Weather systems in tropical Africa are strongly coupled to convection across a range of scales, from individual thunderstorms to organized squall lines and MCSs
- These convective systems are linked to large-scale synoptic dynamics and also controlled by the stability of the atmosphere, its diurnal fluctuations and interactions with underlying land surface and topography
- Initialization and modeling of these convective weather systems remains a research challenge
- The weather systems over Africa play a key role in determining the weather and climate of other regions through remote teleconnections, at both intra-seasonal time scales and even after 3 days of forecast

Needed

- Research to show variability over Africa on sub-seasonal timescales of weeks (e.g. equatorial Kelvin waves) to months (e.g. MJO) that can modulate precipitation
- Observations to
  - initialise forecasts,
  - understand the physical and dynamical processes of specific weather phenomena,
  - Study their potential predictability
  - Help evaluate and improve numerical models

Some Past large field experimental

- GARP Atlantic Tropical Experiment (GATE) operated out of West Africa in 1974
  - Objective: To understand the tropical atmosphere and its role in the global circulation
- African Monsoon Multidisciplinary Analyses (AMMA) field campaign in 2006
  - Objective: To study the West African Monsoon physical processes and predictability

Smaller scale field experiment – to study specific aspects of African weather systems, such as

- Saharan Heat Low (e.g. Fennec),
- Role of dust/aerosols in weather and climate (BodEX, SAMUM, GERBILS)
- JET2000 demonstrated the value of sonde profiling for NWP through the use of dropsonde data from research aircraft

Fundamental Elements of a Deterministic NWP Forecast

- Observations – for initialization and evaluating NWP models
- Data assimilation
- Land
- Ocean
- Numerical model

Ensemble Forecasting

- Key technique in providing risk assessment for severe and hazardous weather
- Ensembles being used in data assimilation techniques

- Fig 3 shows the spatial distribution of some of the quality controlled observations used to initialize the UKMO Model on a single day at 0000 UTC on 27 February 2013.

Data Assimilation (DA)

- DA is the combination of observations with a "first guess" or "background" of the initial state from a previous NWP short-range forecast (usually 6 hours), which provides data on the regular model grid. The combination of the observations and model background is done in a statistically optimal way that takes account of known errors in both data sets.
- The outcome of the combination is a balanced initial state that is the best estimate of the current temperature, Moisture, winds, soil state etc. on a regular grid that can be used in numerical models of the atmosphere, land and ocean to provide a forecast.
- DA techniques have evolved from simple optimal interpolation techniques (1960s to 1980s), to more complex variational assimilation (3D-Var and 4D-Var), Kalman filtering and ensemble techniques
- At the heart of many DA systems (e.g. Successive Correction Method (SCM), Optimum Interpolation (OI), 3D-Var, and Kalman Filtering (KF)) is an analysis equation

$$x_a = x_b + W[y_o - H(x_b)]$$

x represents a model state and y an observation.

African Monsoon Multidisciplinary Analysis

ACMAD

WMO

Data Assimilation cont'd

- The analysis equation states that the model analysis (x_a) is the background state (x_b) plus some observation increments or "innovations", y_o – H(x_b), which measure the difference between the observation (y_o) and the background (Fig 10.4).
- x and y are large vectors
- The forward operator , H, which could be a radiative transfer model to convert temperature and moisture to radiances, is used to convert the background to the same measurement space as the observation. The term, W, is an optimal weight based on statistical estimates of the typical errors (error covariances) of the model and the observations.
- xxx

African Monsoon Multidisciplinary Analysis

ACMAD

WMO

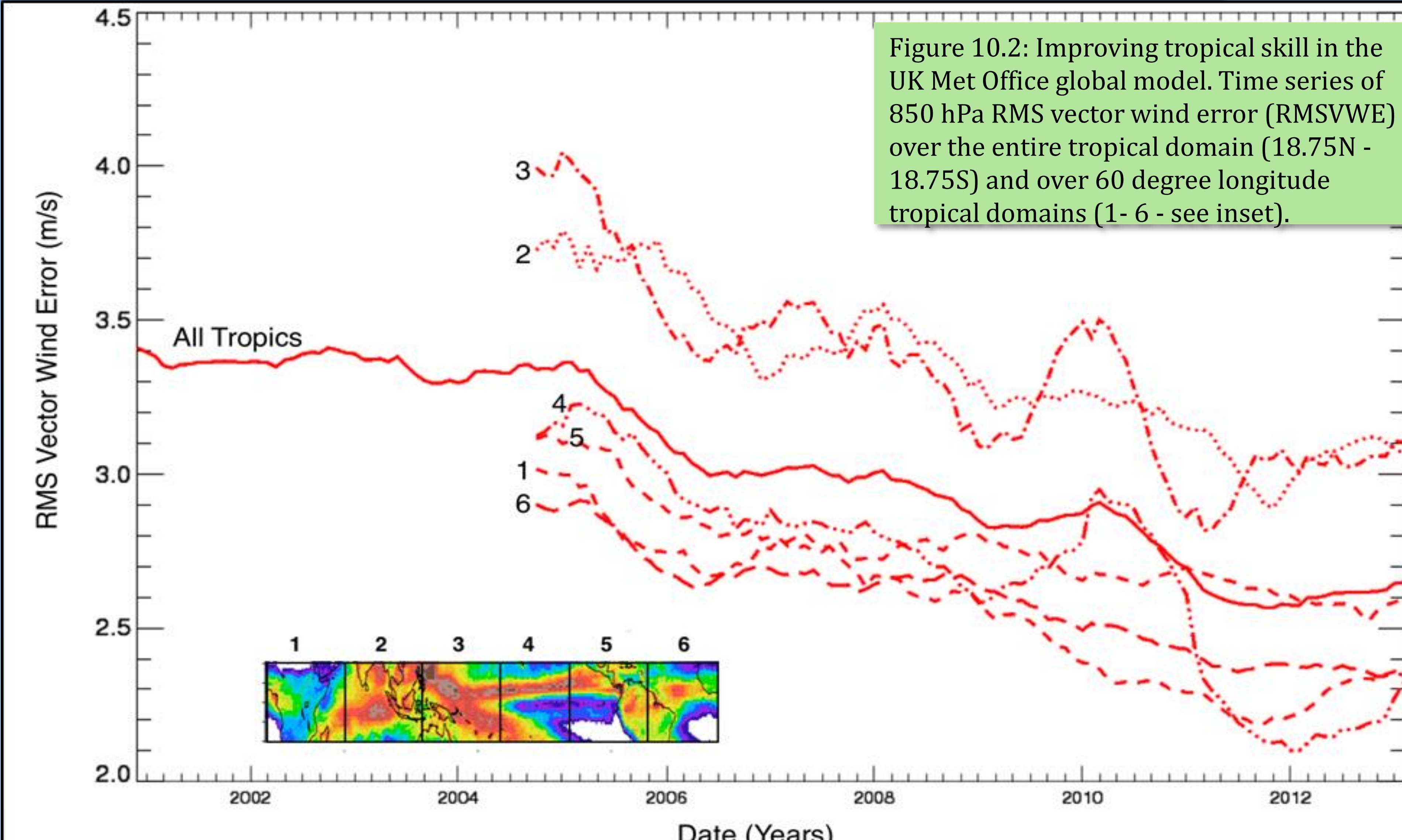

Figure 10.2: Improving tropical skill in the UK Met Office global model. Time series of 850 hPa RMS vector wind error (RMSVWE) over the entire tropical domain (18.75N - 18.75S) and over 60 degree longitude tropical domains (1- 6 - see inset).

Chapter 10: *Numerical Weather Prediction over Africa* – Lead author: Sean Milton

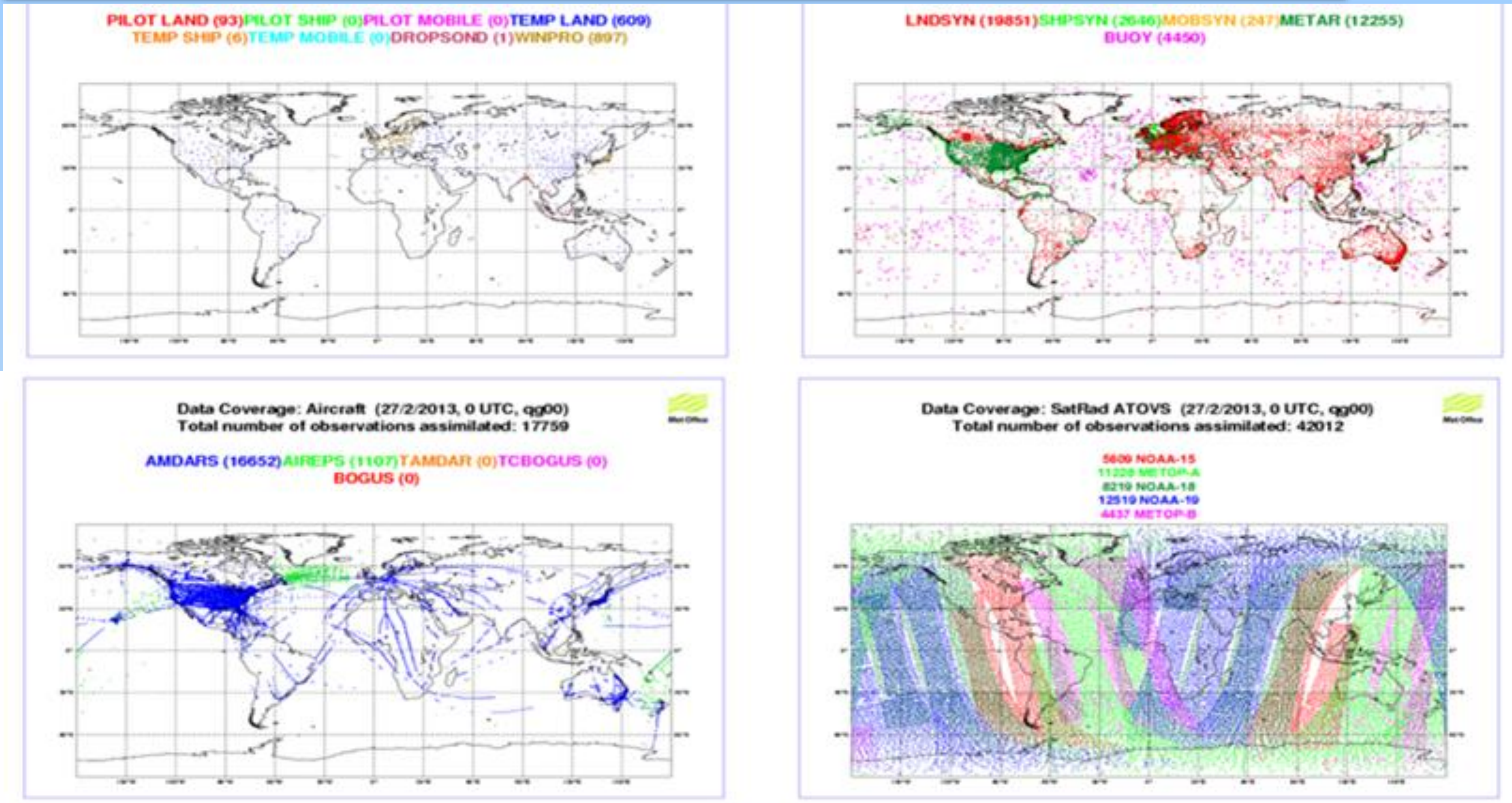

Figure 10.3/1: Data coverage of quality controlled observations used in the Met Office data assimilation to initialise the global NWP forecast at 0000 UTC on 27 February 2013.

Chapter 10: *Numerical Weather Prediction over Africa* – Lead author: Sean Milton

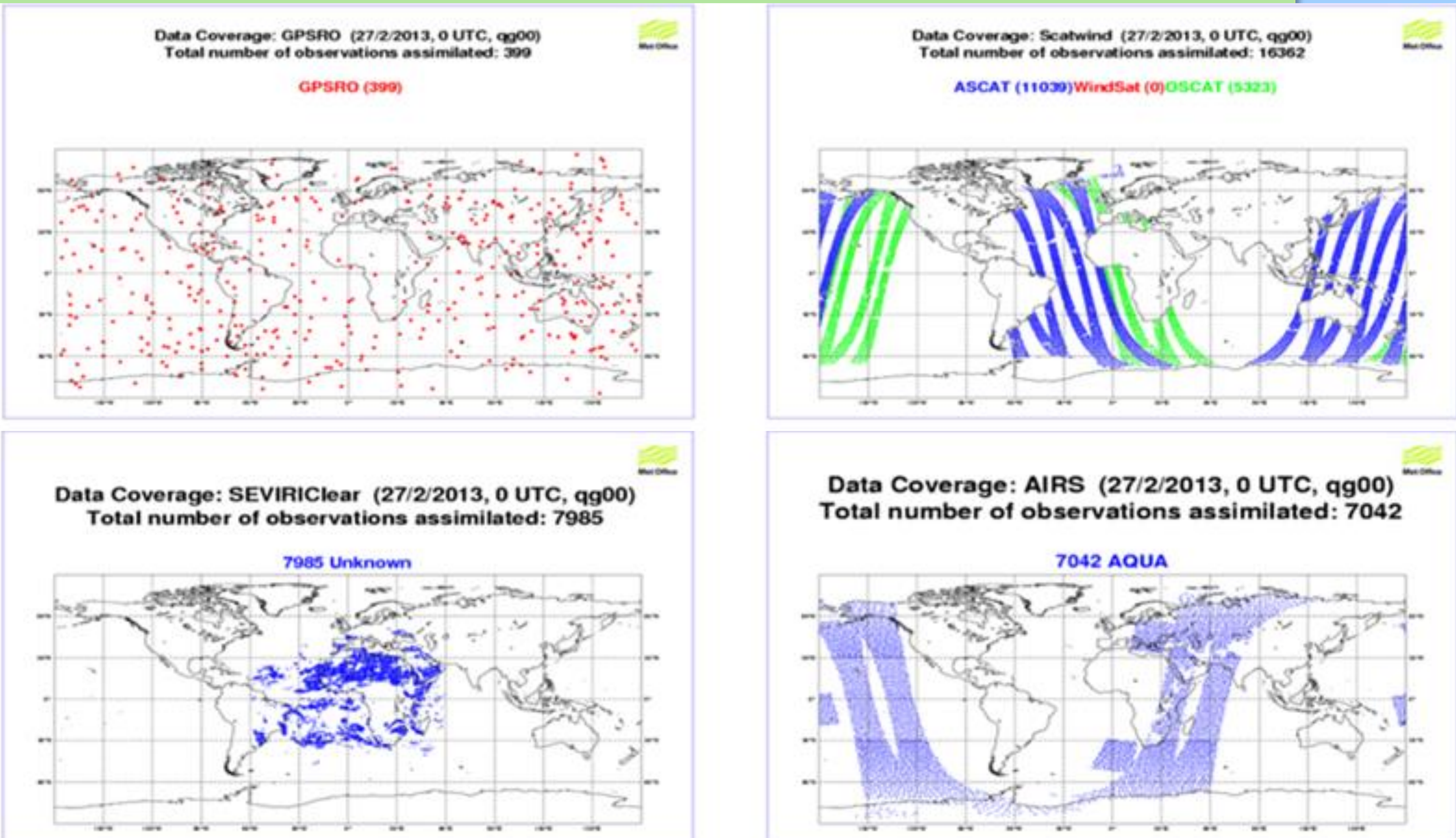

Figure 10.3/2: Data coverage of quality controlled observations used in the Met Office data assimilation to initialise the global NWP forecast at 0000 UTC on 27 February 2013.

Chapter 10: *Numerical Weather Prediction over Africa* – Lead author: Sean Milton

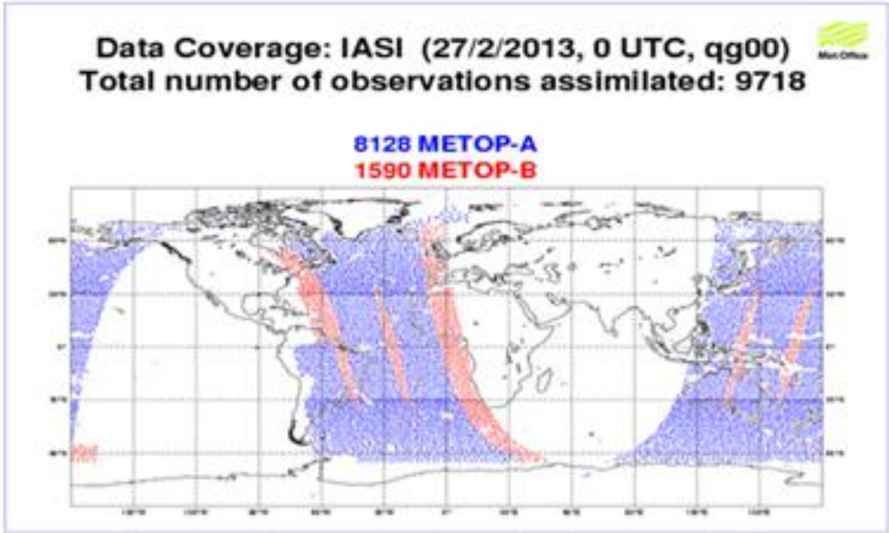

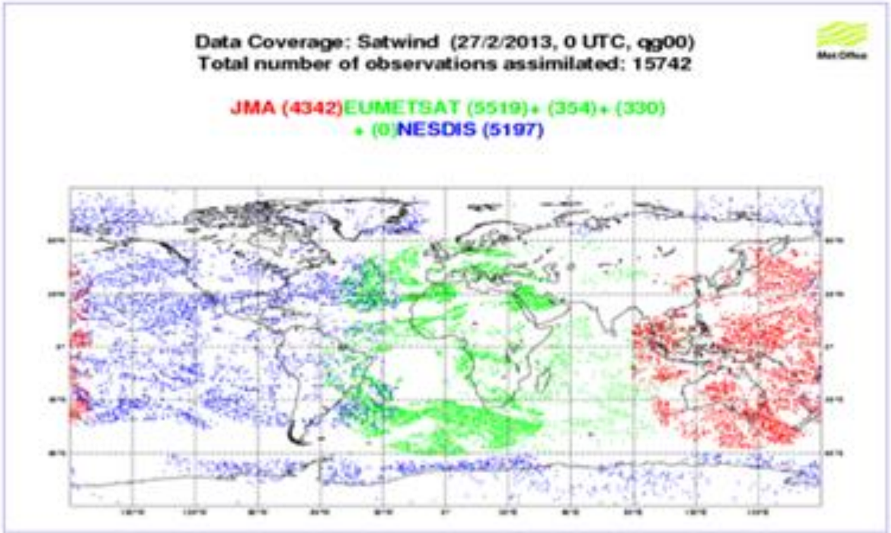

Figure 10.3/3: Data coverage of quality controlled observations used in the Met Office data assimilation to initialise the global NWP forecast at 0000 UTC on 27 February 2013.

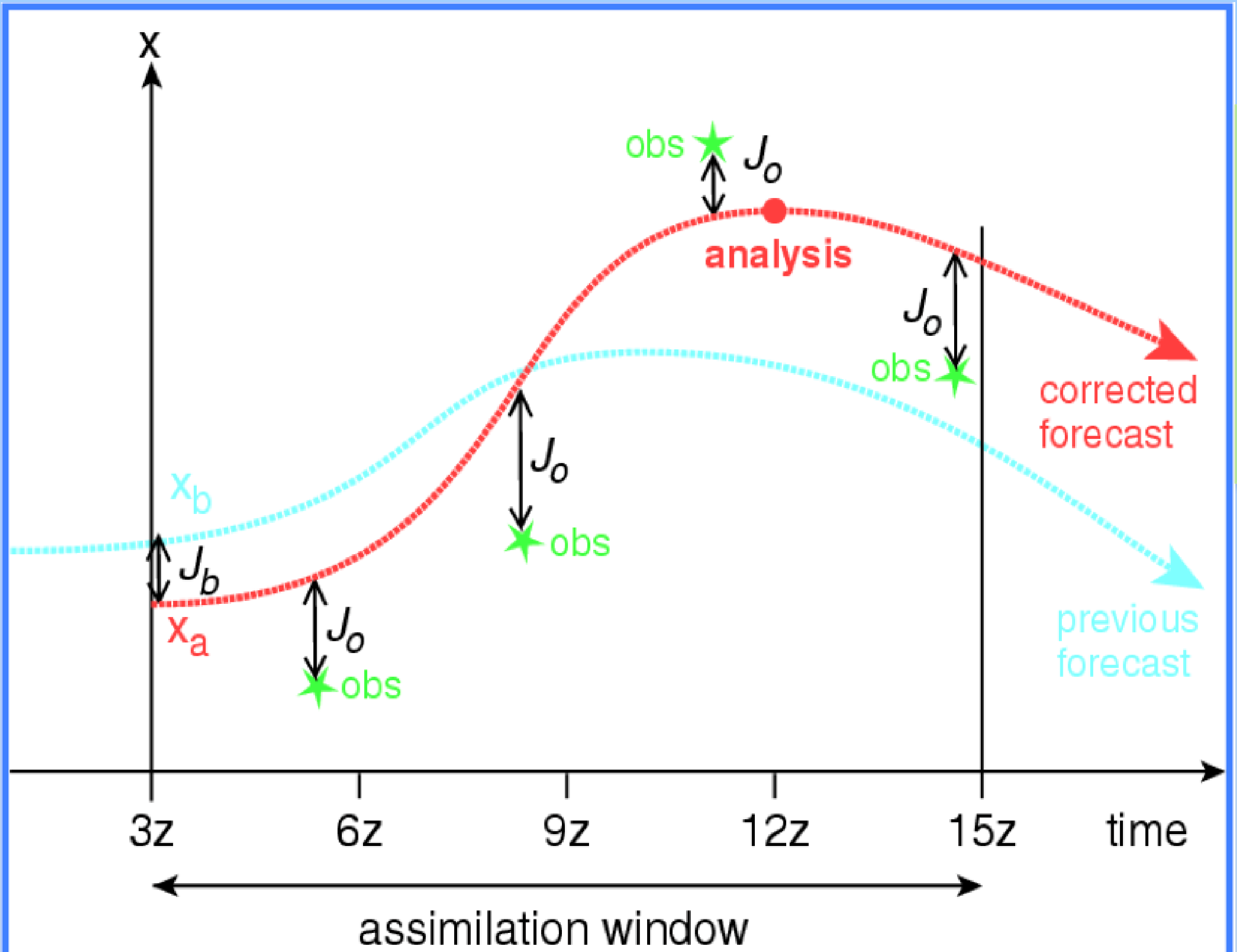

Figure 10.4: Schematic of the 4 dimensional variational data assimilation process (from Bouttier and Courtier, 1999). This shows a 12-hour assimilation window.

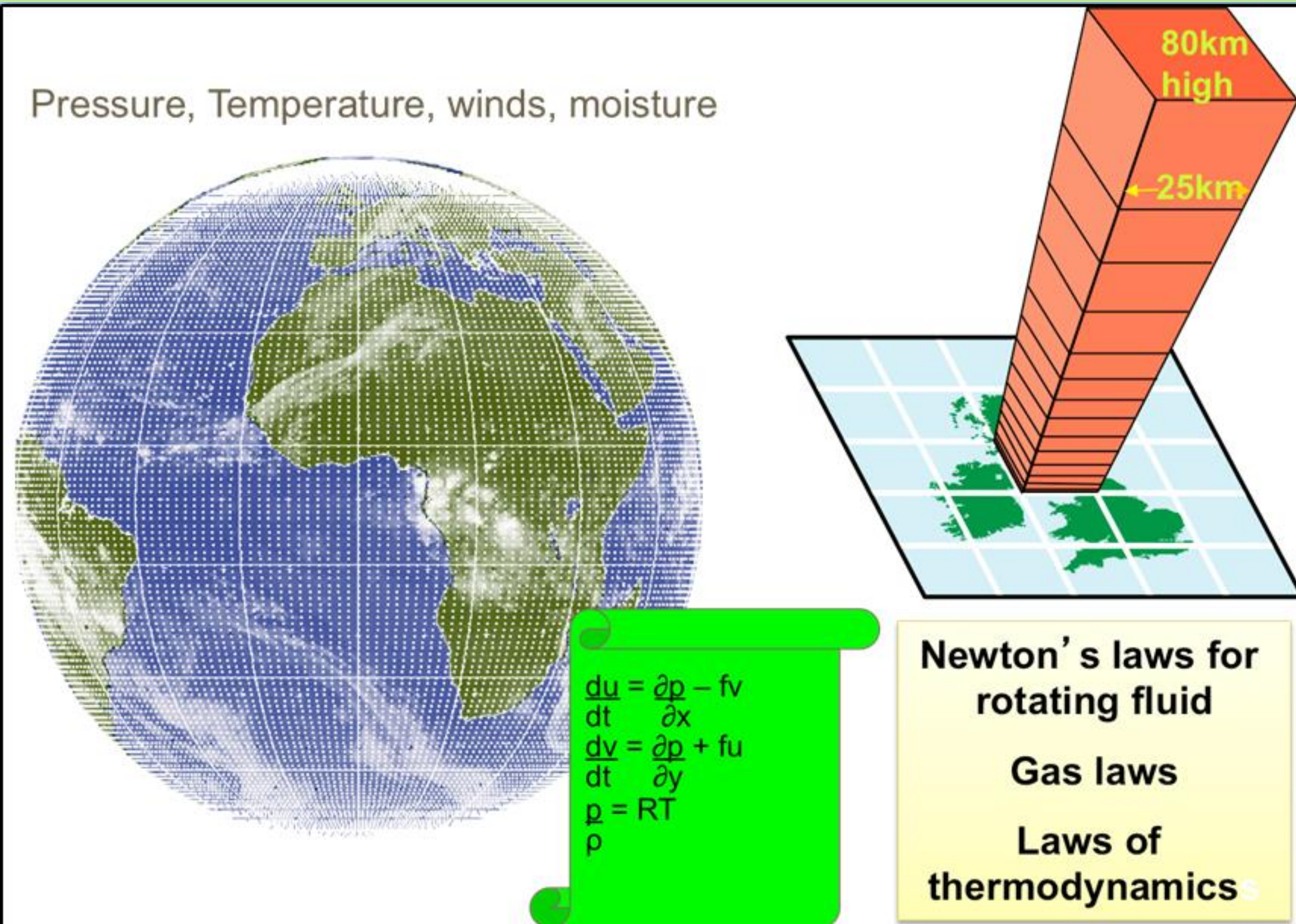

Figure 10.5: Model horizontal and vertical grids on the sphere used to solve the fluid equations to provide a numerical weather forecast. The dimensions and grid spacings are from the Met Office Unified Model (MetUM) used for global NWP (Circa August 2013).

Chapter 10: ***Numerical Weather Prediction over Africa*** **– Lead author: Sean Milton**

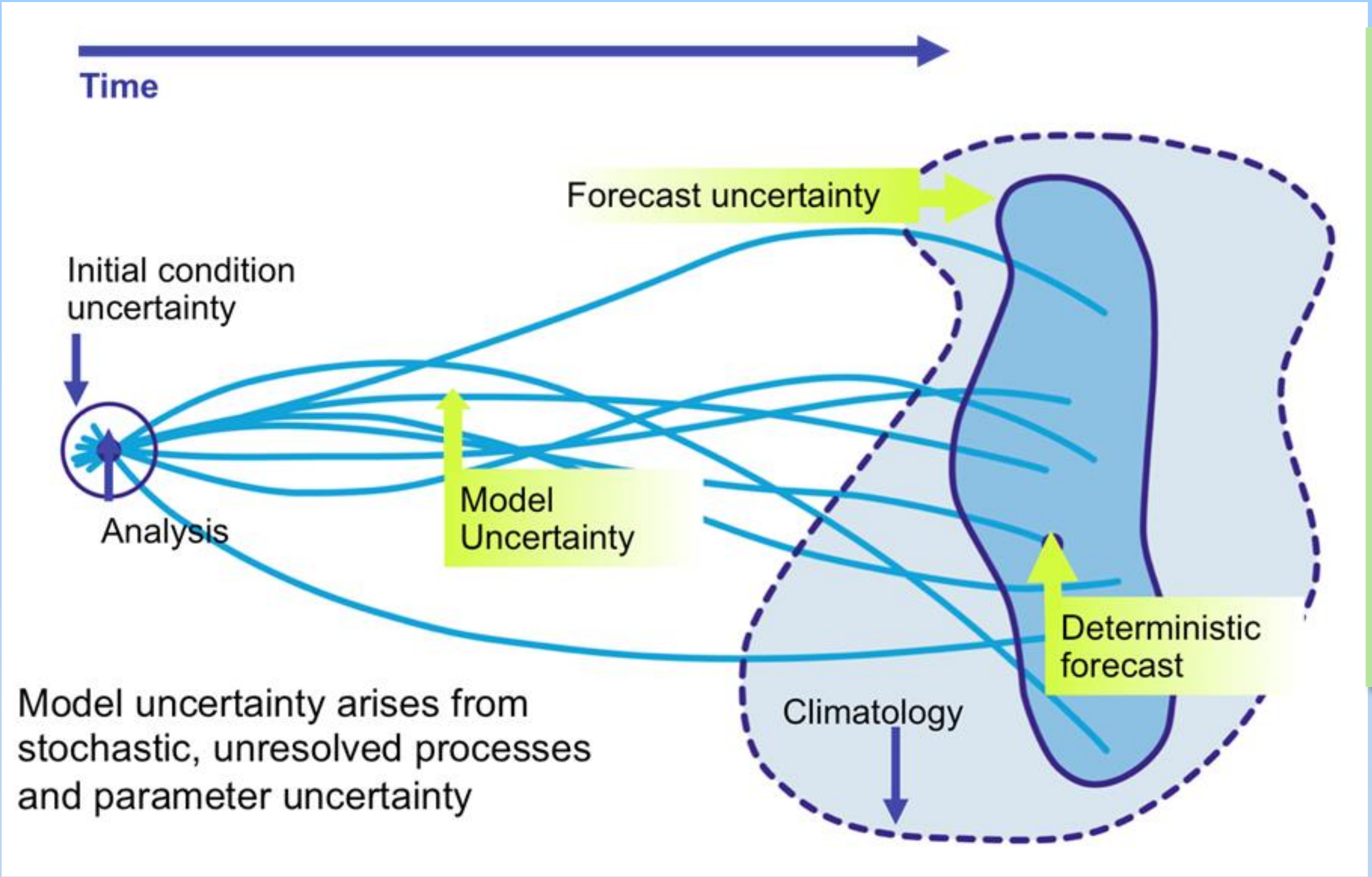

Figure 10.6: Schematic of the ensemble prediction process. Two types of uncertainty are represented, the initial condition uncertainty given by perturbations to the initial analysis and the model uncertainty.

African Monsoon Multidisciplinary Analysis

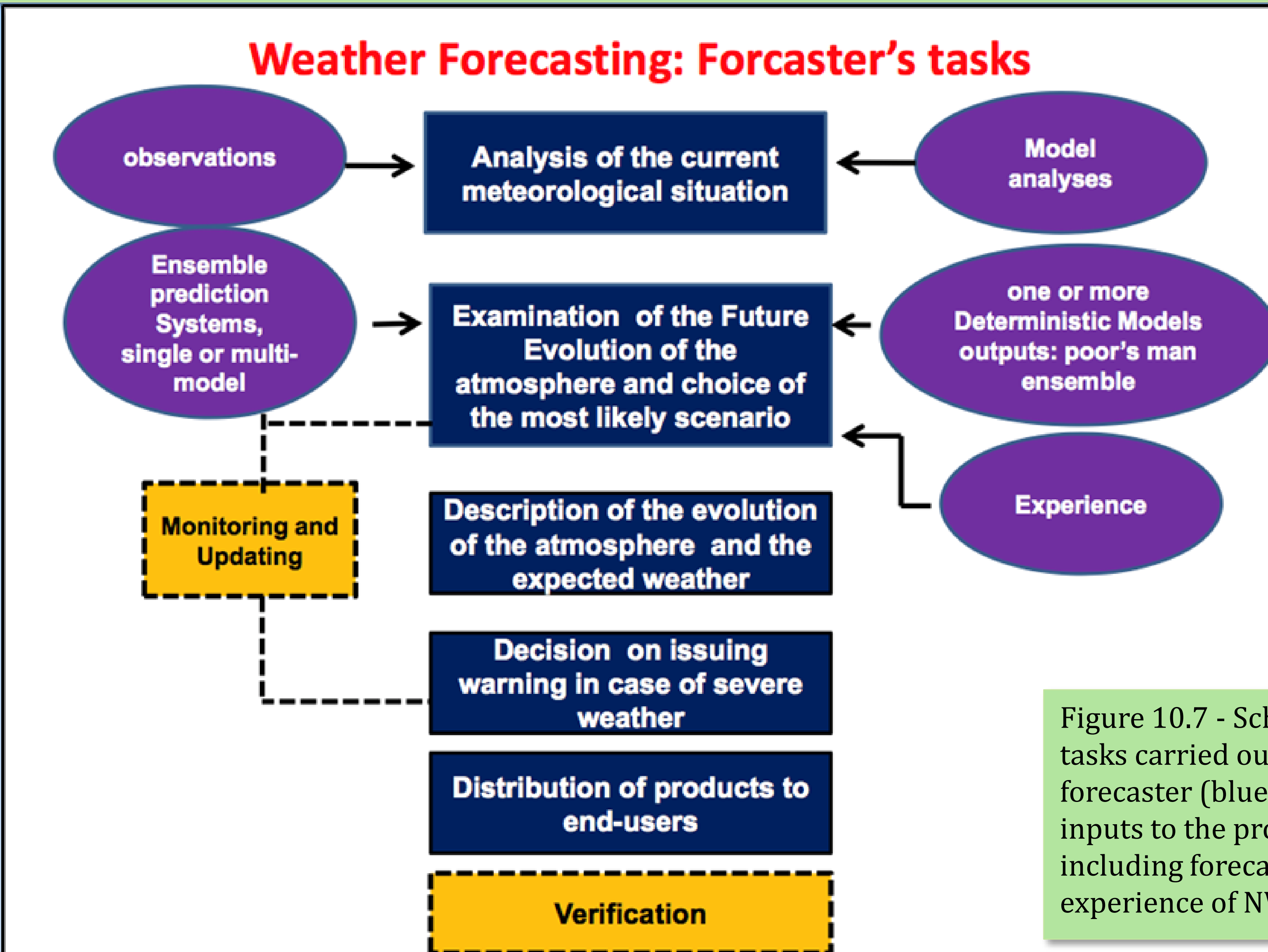

Figure 10.7 - Schematic of typical tasks carried out by the weather forecaster (blue boxes) and the NWP inputs to the process (Purple ovals - including forecaster knowledge and experience of NWP characteristics).

C… – Lead author: Sean Milton

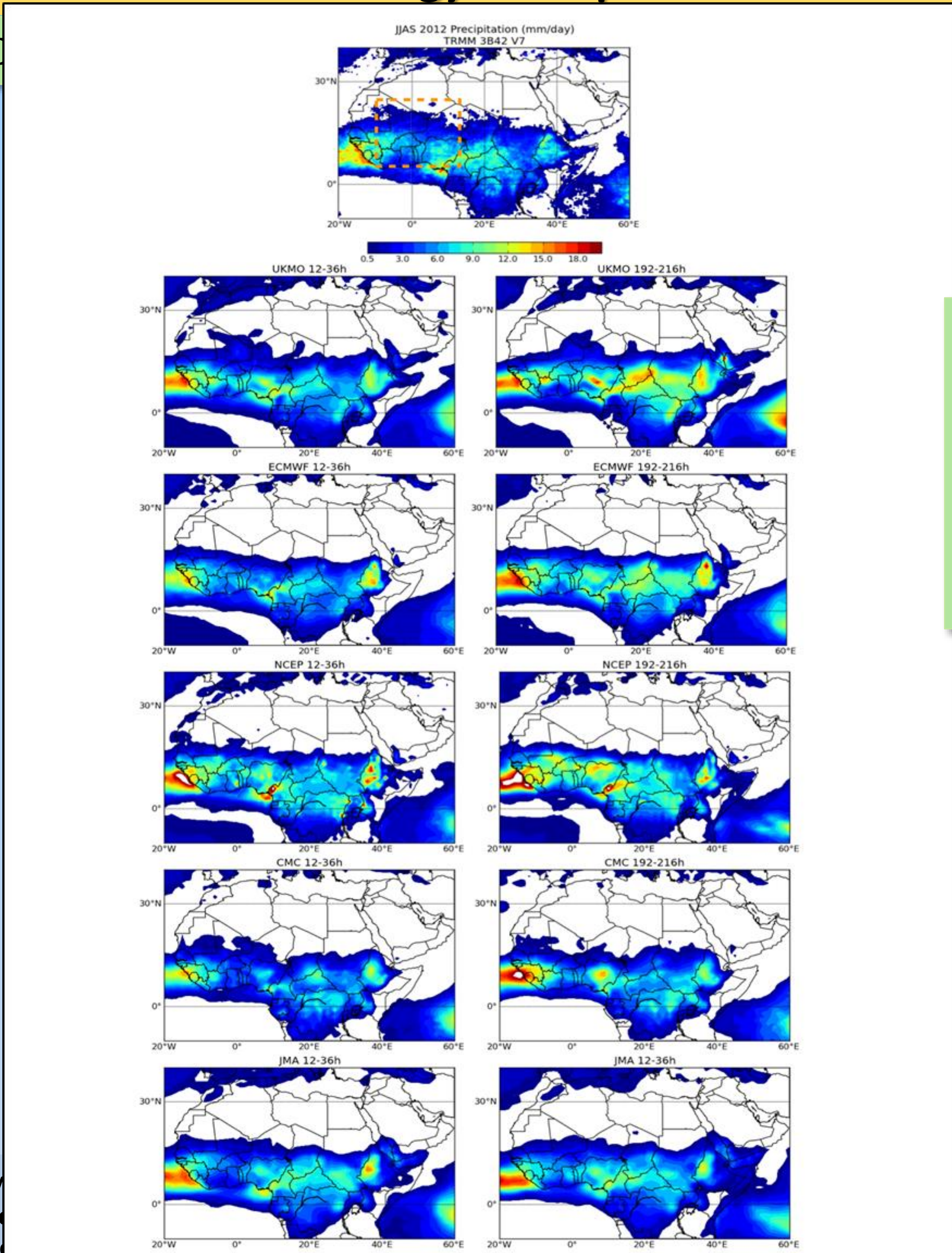

Figure 10.8: Seasonally averaged (June-September 2012) precipitation (mm/day) for TIGGE control forecasts (on 1 degree grid) at 12-36h (left) and 192-216h (8-9 days - right) compared to the TRMM 3B42 version 7 precipitation (top panel – on 0.25 degree grid

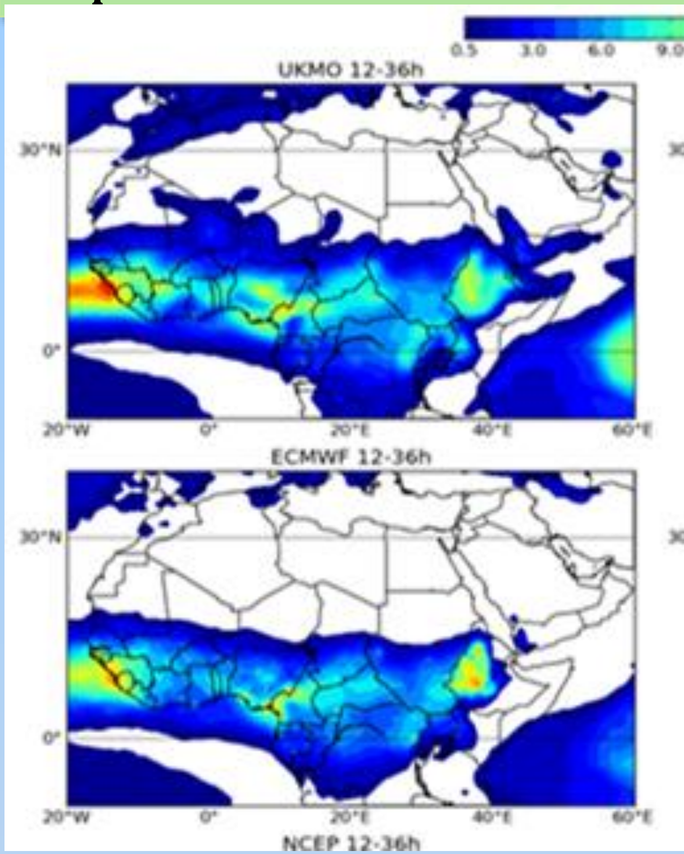

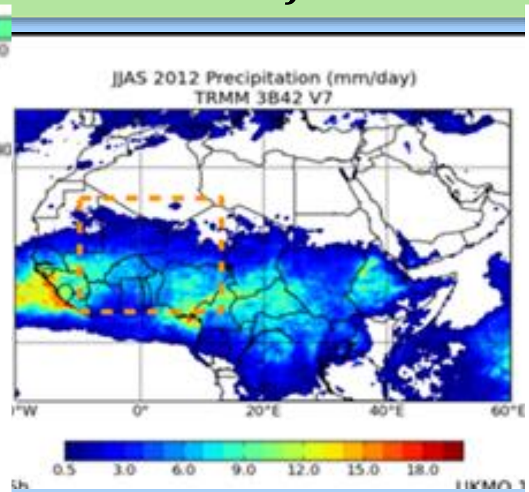

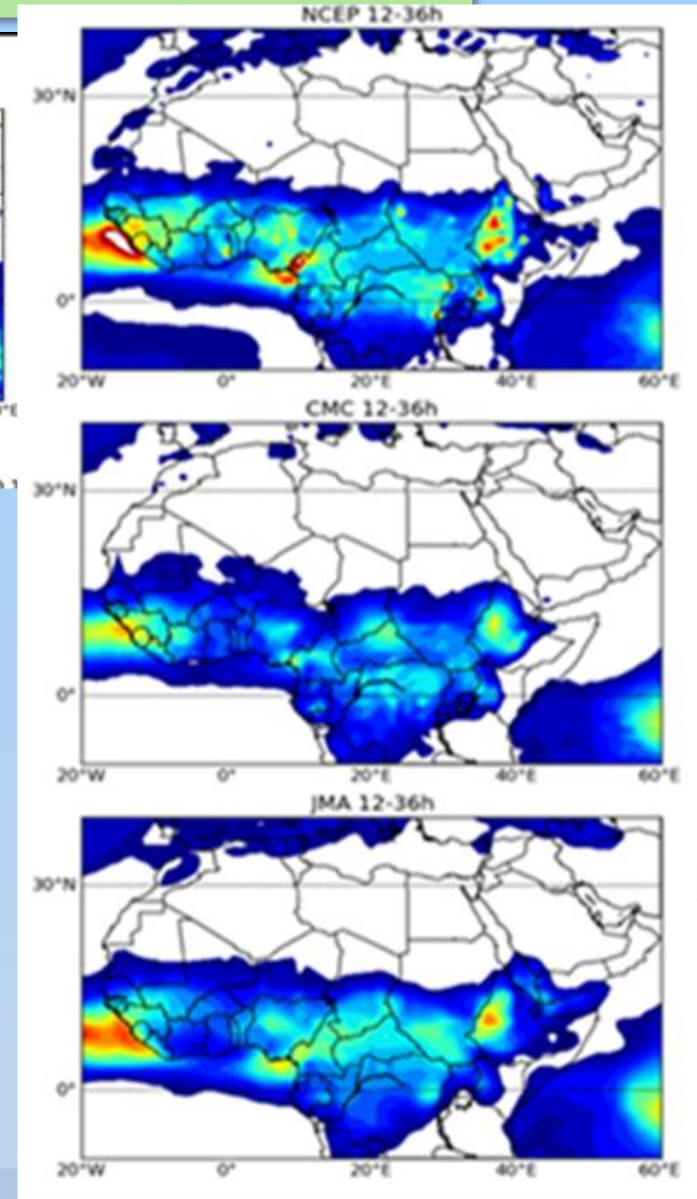

Figure 10.8: Seasonally averaged (June-September 2012) precipitation (mm/day) for TIGGE control forecasts (on 1 degree grid) at 12-36h compared to the TRMM 3B42 version 7 precipitation (centre panel – on 0.25 degree grid

Chapter 10: *Numerical Weather Prediction over Africa* – Lead author: Sean Milton

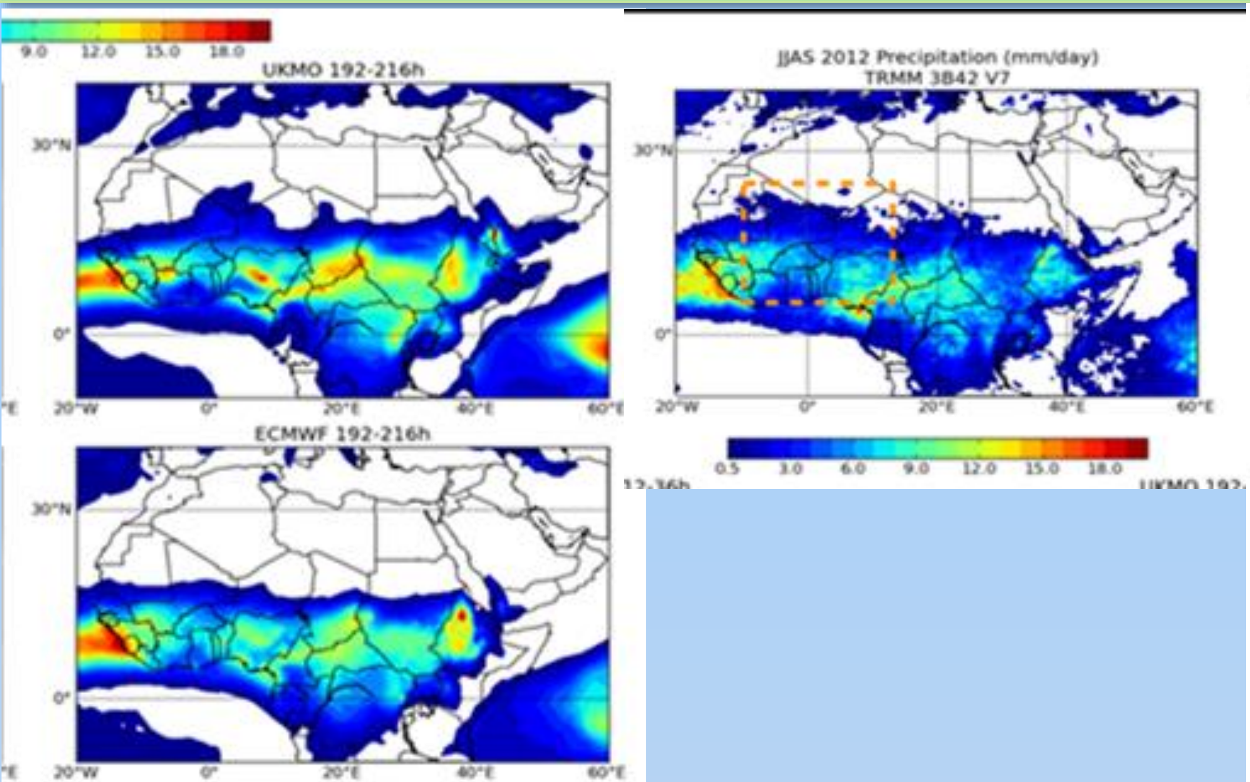

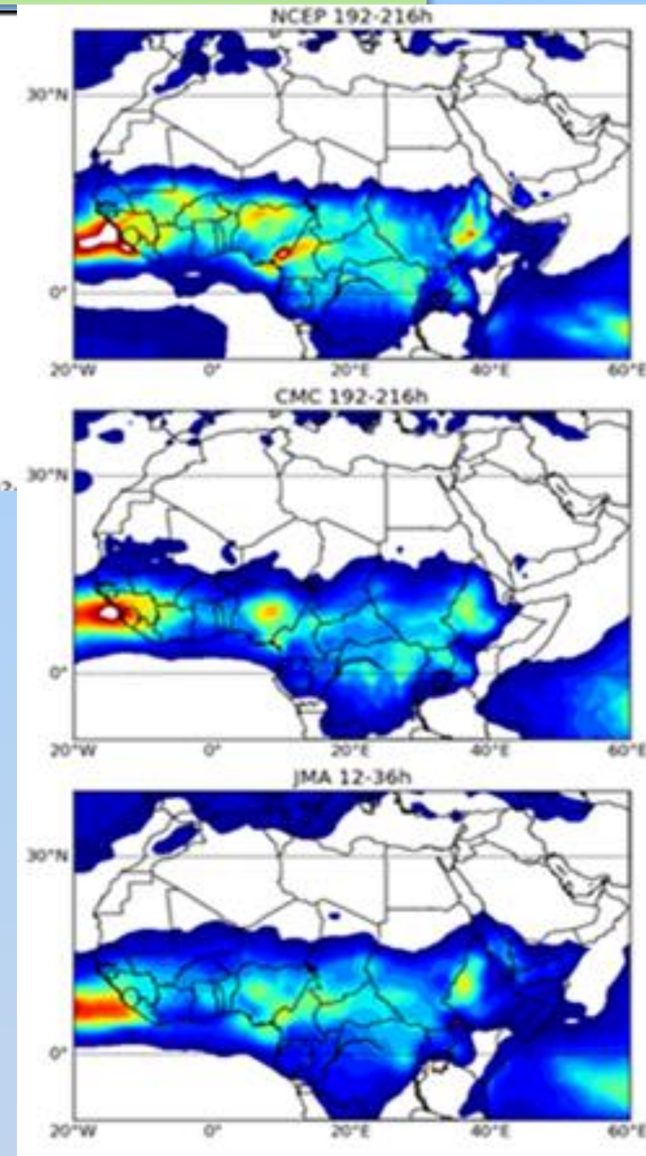

Figure 10.8: Seasonally averaged (June-September 2012) precipitation (mm/day) for TIGGE control forecasts (on 1 degree grid) at 192-216h (8-9 days) compared to the TRMM 3B42 version 7 precipitation (centre panel – on 0.25 degree grid

Meteorology of Tropical West Africa: The Forecasters' Handbook
Editors: D J Parker and M Diop-Kane

African Monsoon Multidisciplinary Analysis
ACMAD
WMO

Chapter 10: *Numerical Weather Prediction over Africa* – Lead author: Sean Milton

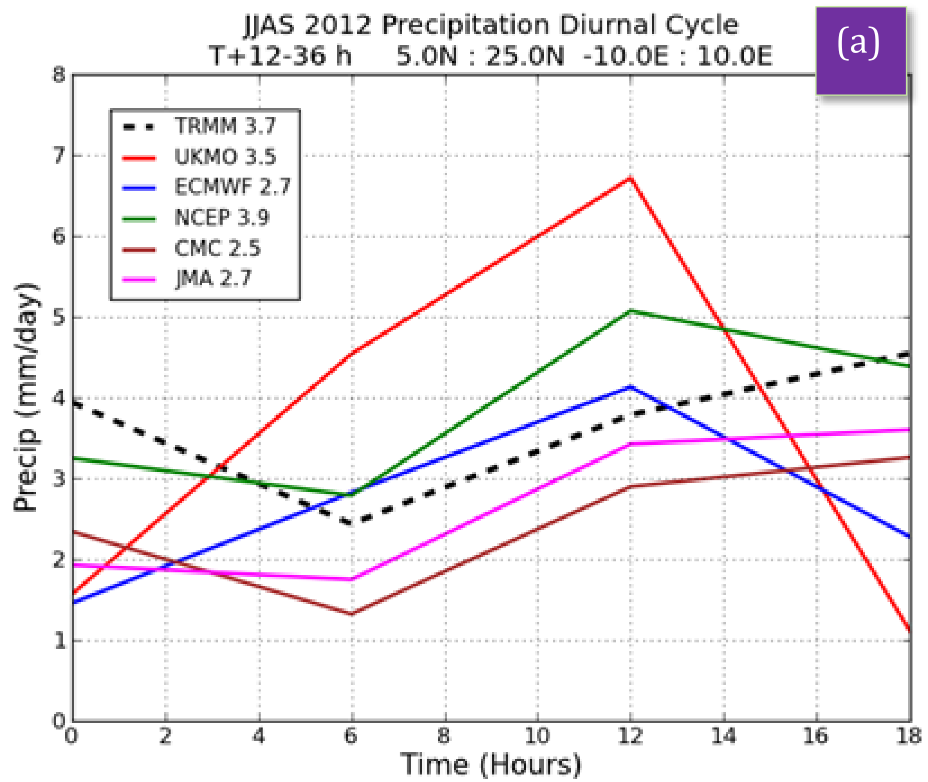

Figure 10.9: Seasonal mean precipitation (mm/day) as a function of the diurnal cycle for (a) TIGGE control forecasts (6-hour sampling) averaged over the domain (5N-25N, 10W-10E) shown in Figure 10.8

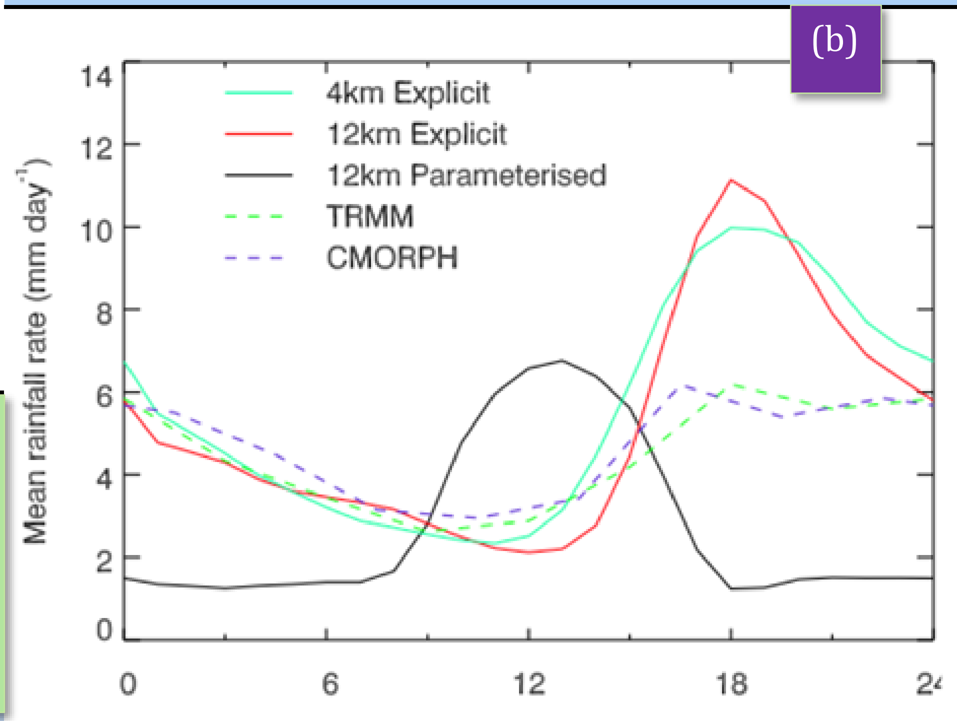

and (b) diurnal cycles of precipitation (mm/day) over West Africa for ob-servational estimates from TRMM and CMORPH datasets compared to a 12 km simulation of the Met Office Unified Model with parameterized convection and 12 km and 4 km simulations with explicit convection .

(Reproduced from Fig. 1(a) of Marsham et al., 2013(a)

Chapte

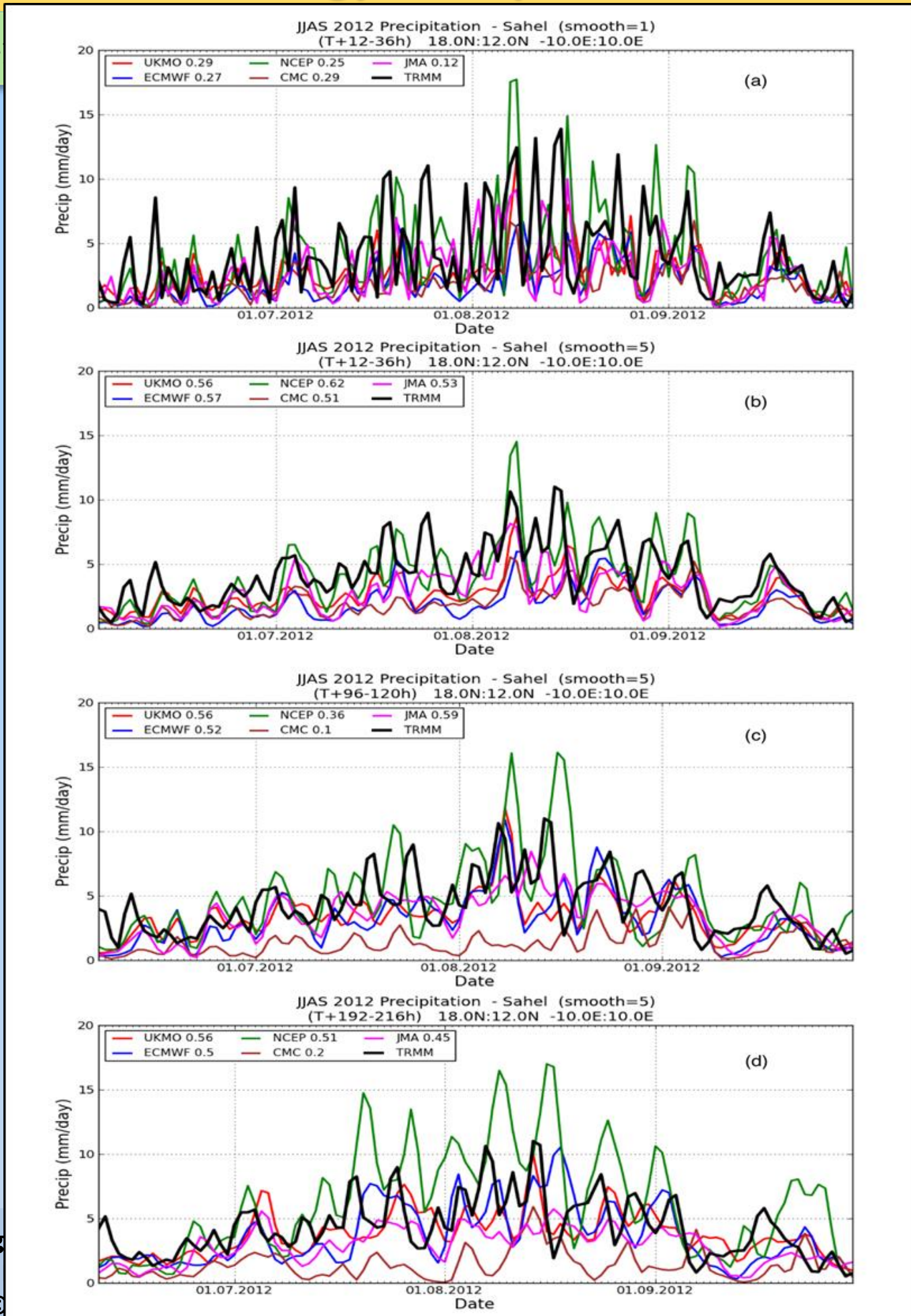

Lead author: Sean Milton

Figure 10.10: Evolution of daily mean precipitation during the June-September 2012 West African Monsoon (10W-10E) season for forecasts at 12-36h and TRMM over (a) the Sahel region (12N-18N), (b) as (a) but for 5-day smoothed precipitation and (c) as (b) but for T+96-120h, (d) as (b) but for T+192-216 (days 8-9 of forecasts). The numerical value in the legends is the time series correlation between each forecast and the TRMM data.

Chapter 10: *Numerical Weather Prediction over Africa* – Lead author: Sean Milton

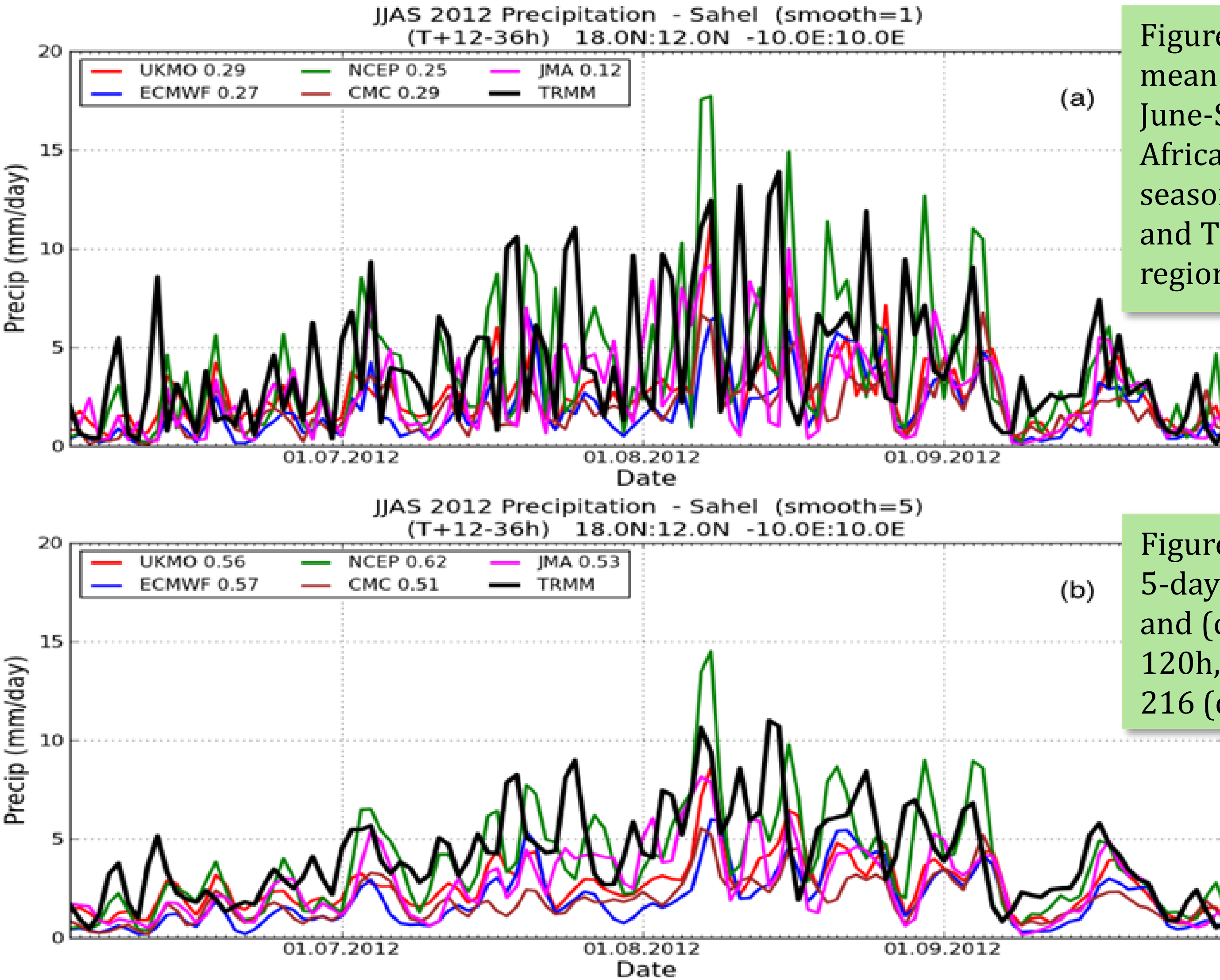

Figure 10.10: Evolution of daily mean precipitation during the June-September 2012 West African Monsoon (10W-10E) season for forecasts at 12-36h and TRMM over (a) the Sahel region (12N-18N).

Figure 10.10: (b) as (a) but for 5-day smoothed precipitation and (c) as (b) but for T+96-120h, (d) as (b) but for T+192-216 (days 8-9 of forecasts).

The numerical value in the legends is the time series correlation between each forecast and the TRMM data.

African Monsoon Multidisciplinary Analysis

ACMAD

WMO

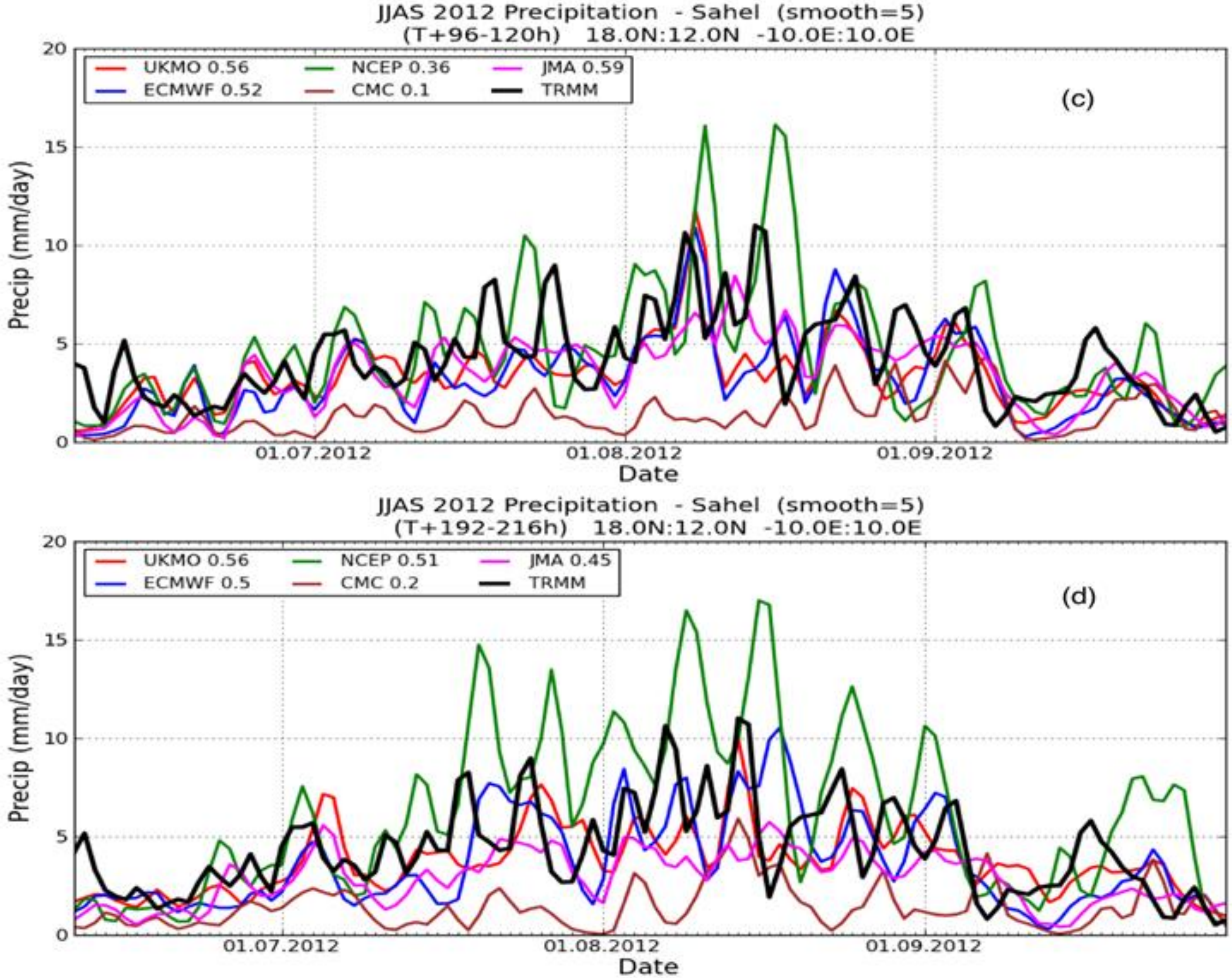

Figure 10.10: Evolution of daily mean precipitation during the June-September 2012 West African Monsoon (10W-10E) season for forecasts at 12-36h and TRMM over the Sahel region (12N-18N), for 5-day smoothed precipitation.

The numerical value in the legends is the time series correlation between each forecast and the TRMM data.

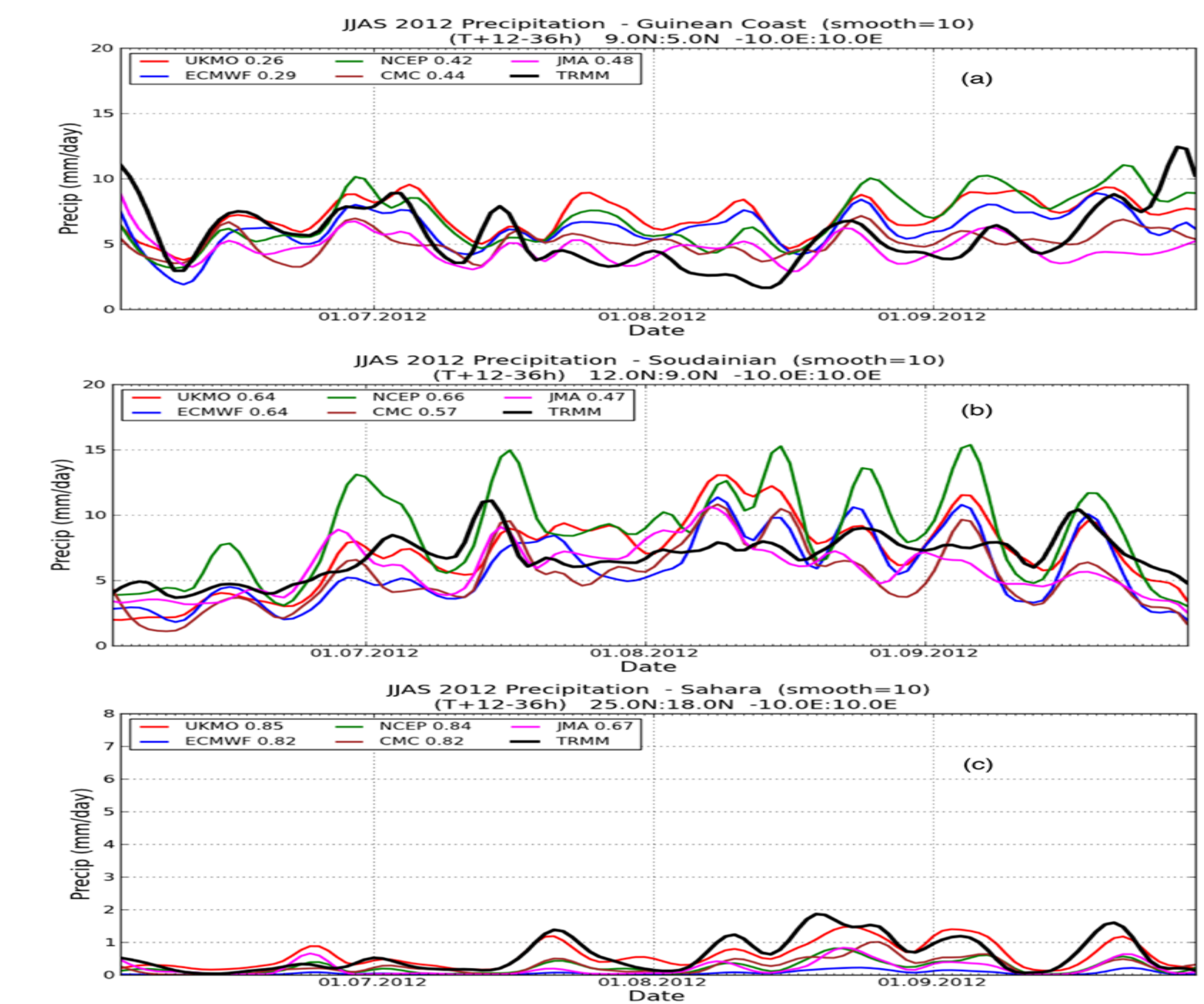

Figure 10.11: Evolution of 10-day smoothed daily mean precipitation during the June-September 2012 West African Monsoon (10W-10E) season for the (a) Guinean Coast region (5N-9N) for (b) Soudanian region (9N-12N) and (c) Sahara (18N-25N)

Chapter 10: *Numerical Weather Prediction over Africa* – Lead author: Sean Milton

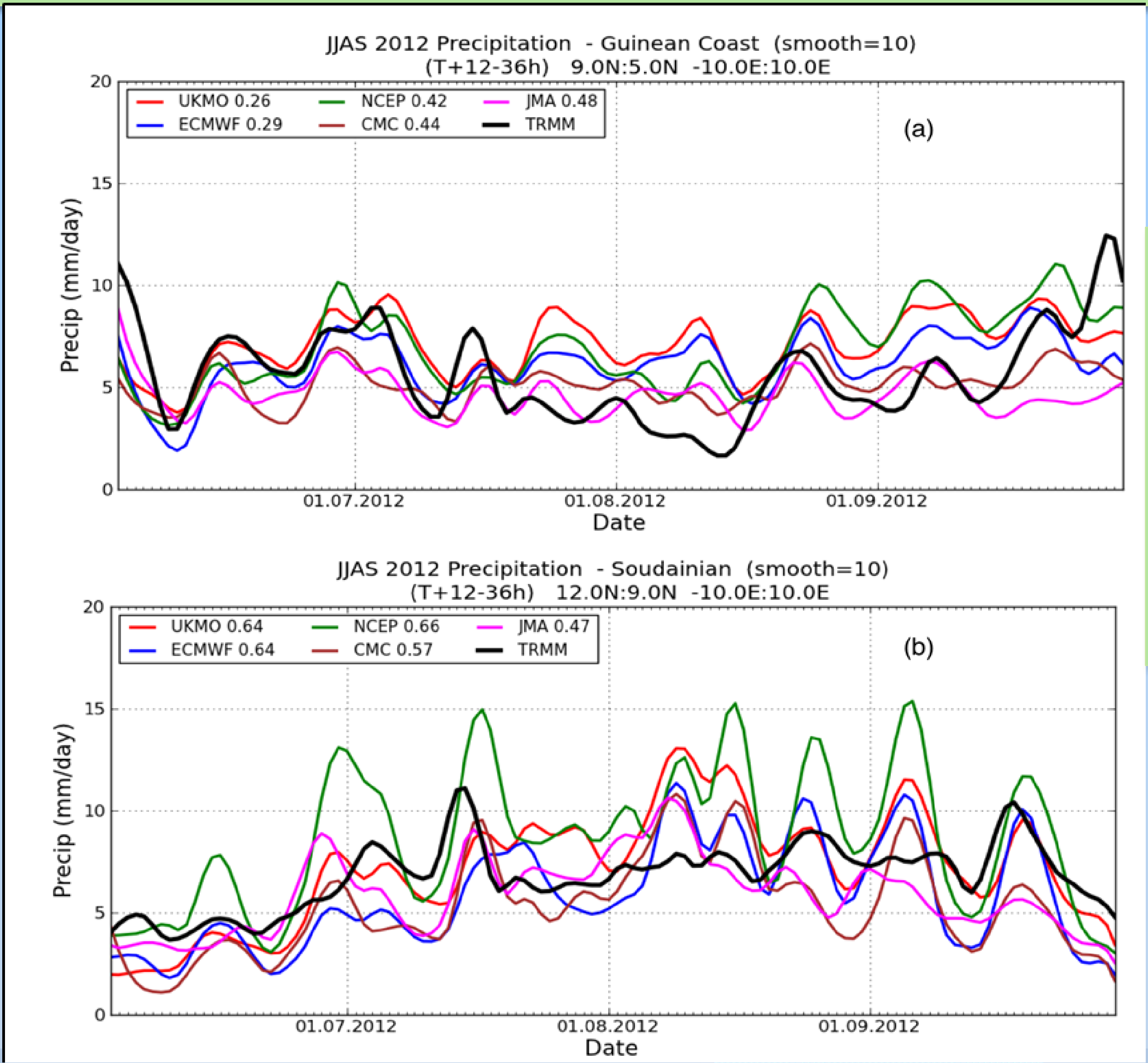

Figure 10.11: Evolution of 10-day smoothed daily mean precipitation during the June-September 2012 West African Monsoon (10W-10E) season for the (a) Guinean Coast region (5N-9N) for (b) Soudanian region (9N-12N) and (c, next slide) Sahara (18N-25N)

African Monsoon Multidisciplinary Analysis

ACMAD

WMO

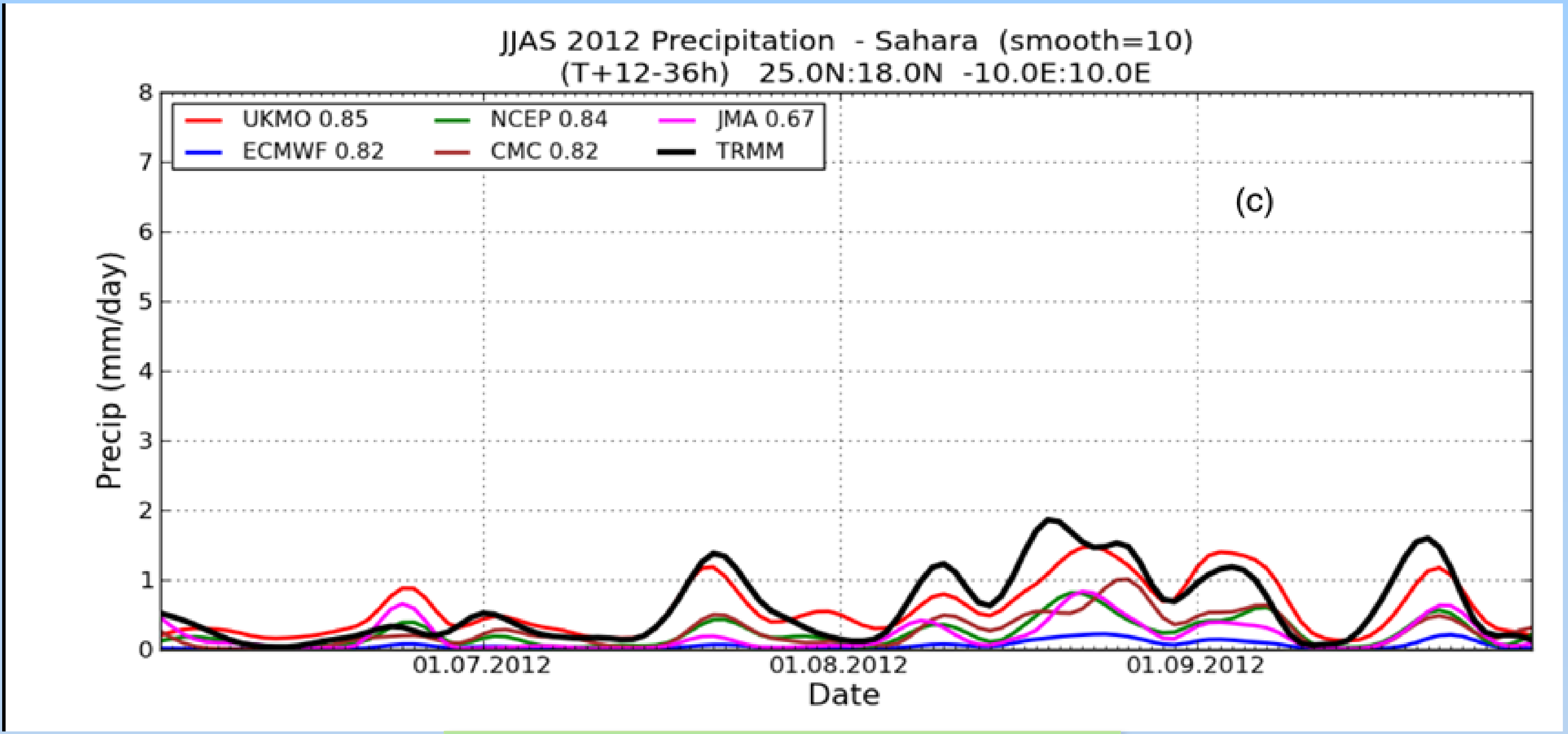

Figure 10.11: Evolution of 10-day smoothed daily mean precipitation during the June-September 2012 West African Monsoon (10W-10E) season for (c) Sahara (18N-25N)

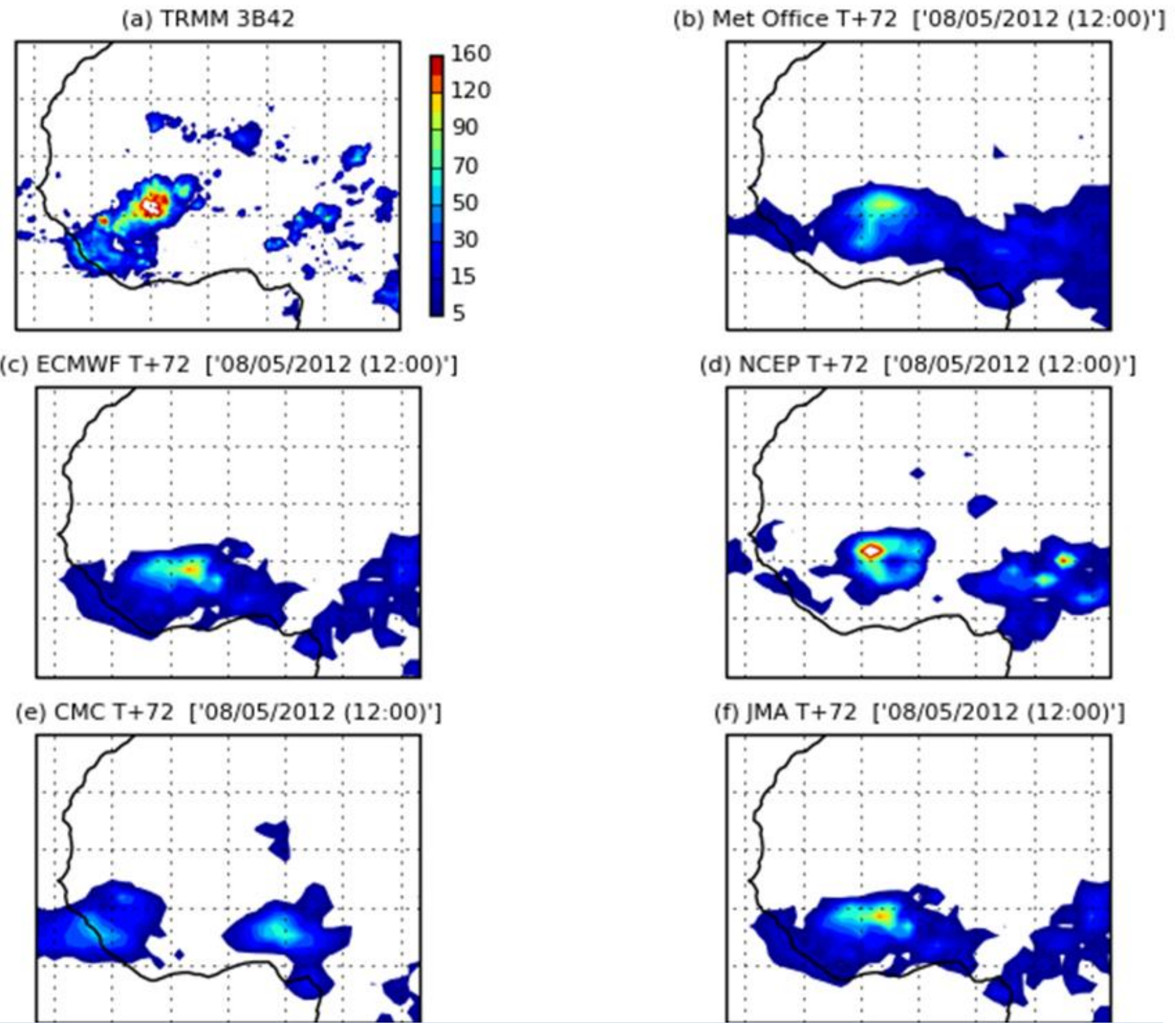

Figure 10.12: Daily accumulated precipitation (mm/day) - Case study for 7-8 August 2012 showing TRMM and TIGGE control (T+48-72h) forecast precipitation accumulation for forecasts initialised at 1200 UTC on 5 August 2012.

Evaporation minus precipitation

Moisture flux divergence

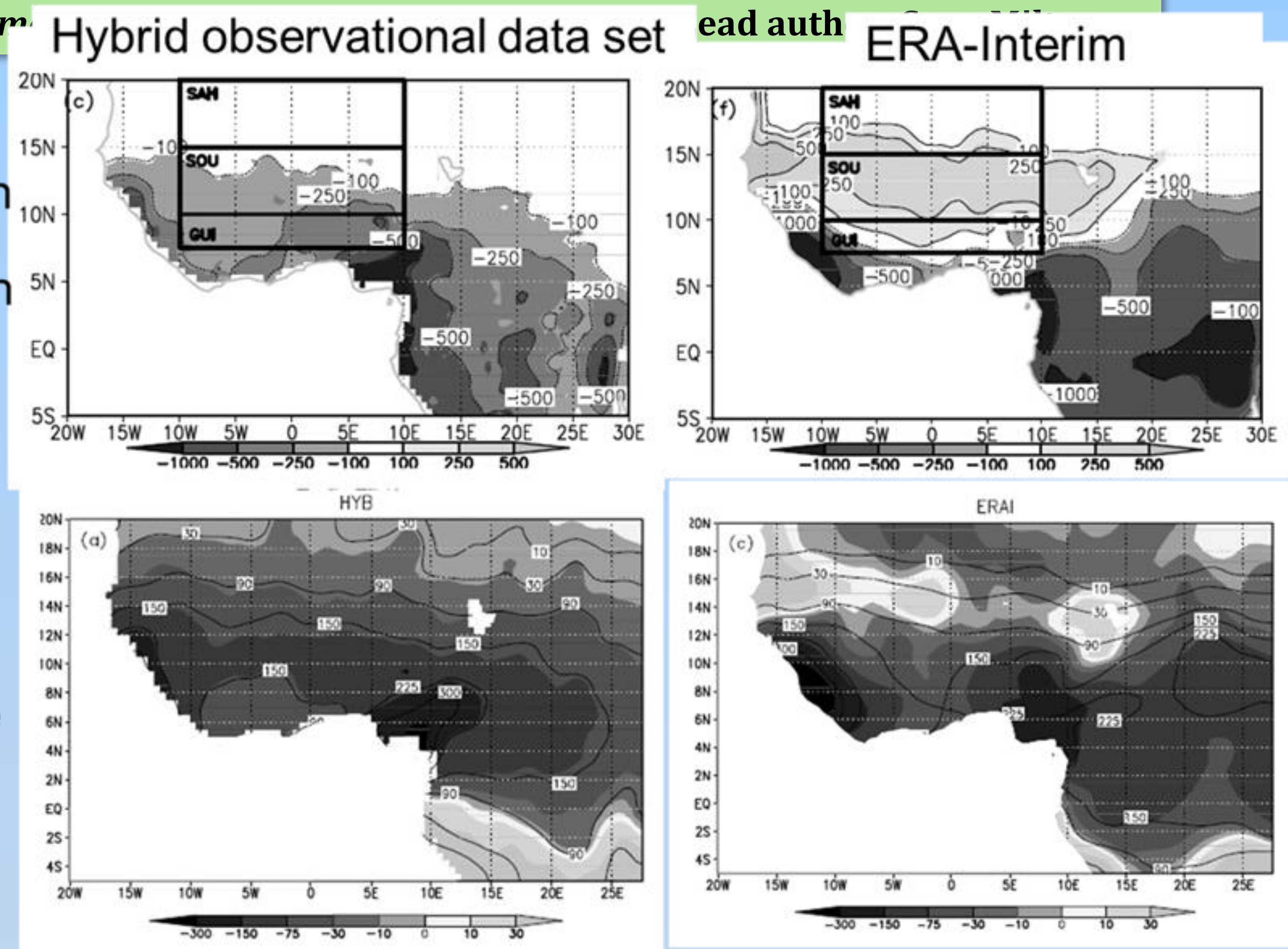

Fig 10.13: Estimates for Evaporation minus Precipitation (top) and Moisture flux divergence (bottom) during August (2002-2007) from the hybrid observational dataset (left) and from ERA-Interim analysis right.

lton

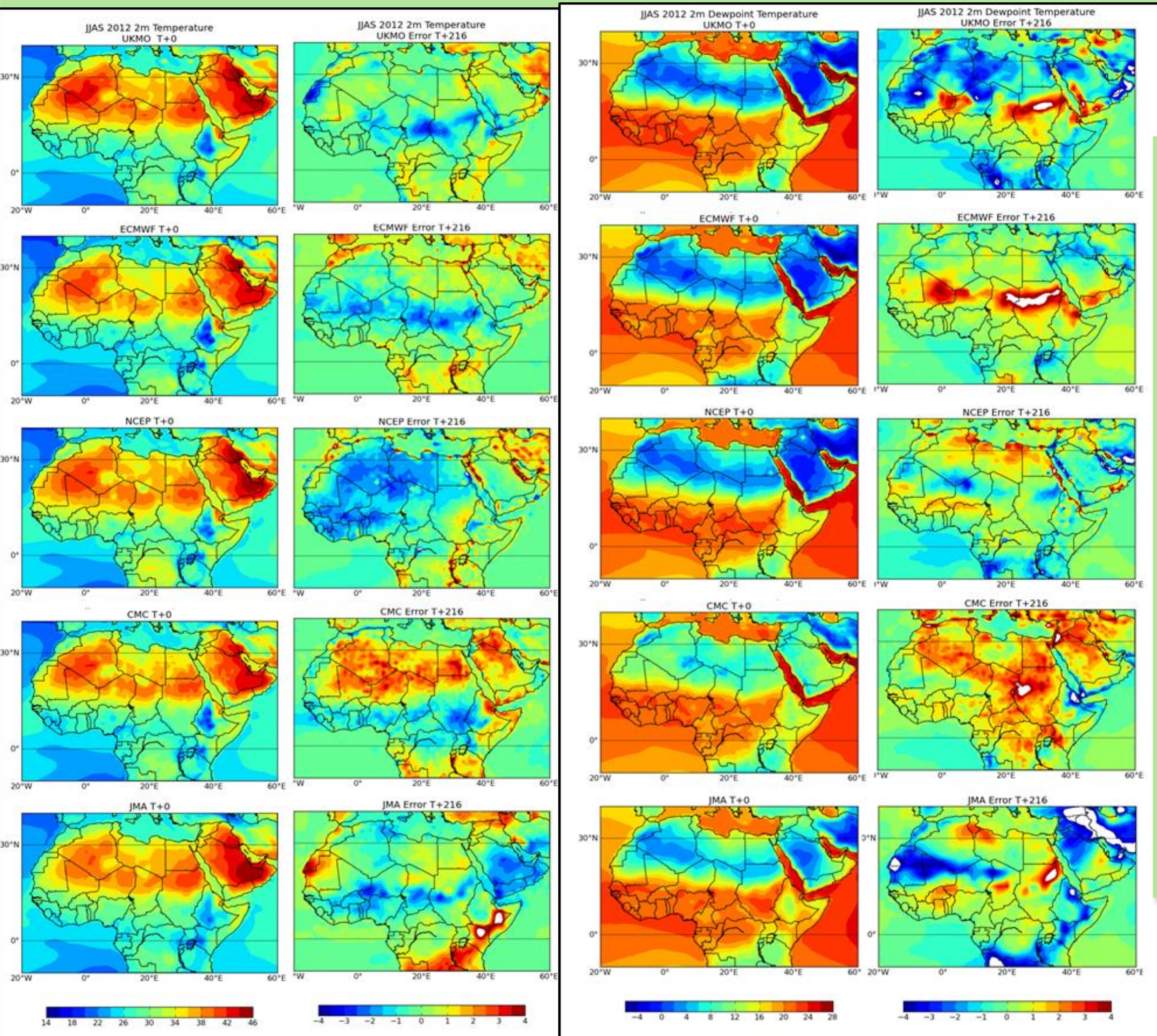

Figure 10.14: Seasonally averaged near surface (2 m) temperatures (column 1) and dewpoint temperatures (column 3) from TIGGE analyses (see Table 10.2) for June-September 2012. The T+216h (day 9) mean model errors/drifts (Forecast - Analysis) are also shown for 2 m temperature (column 2) and 2 m dewpoint temperature (column 4)

WMO

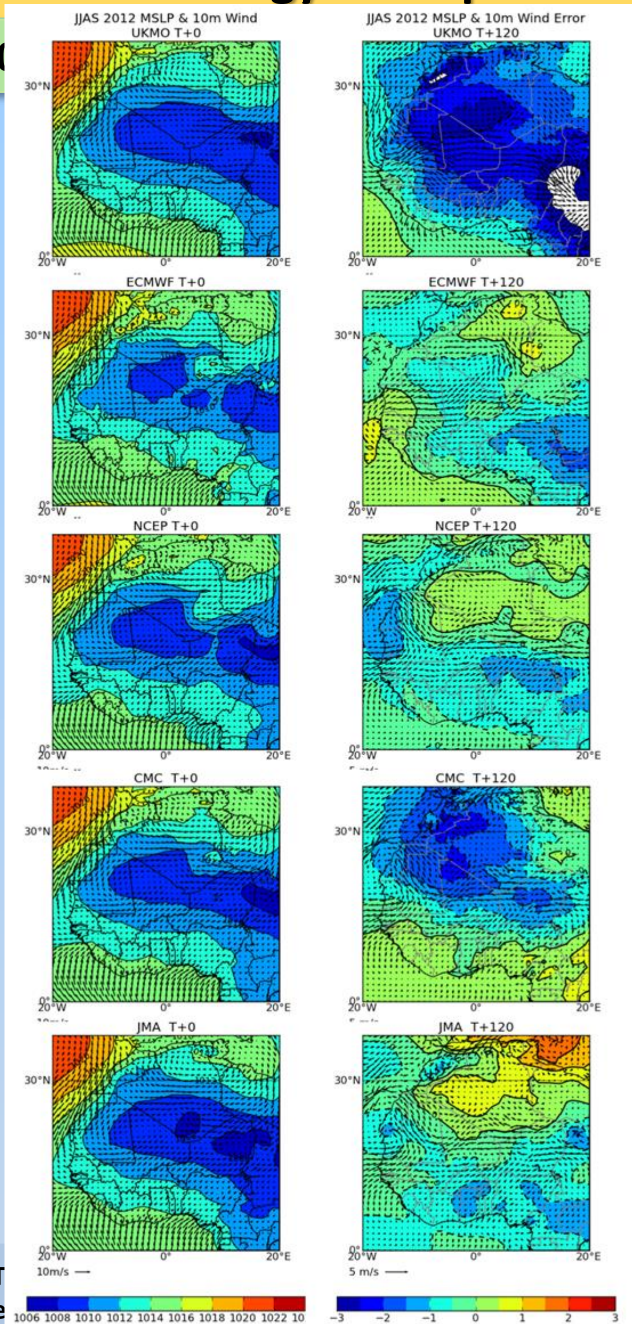

Figure 10.15: Low level monsoon flow (10 m wind vectors) and Saharan heat low (MSLP) for TIGGE analyses (left) and control forecast errors at T+120 (right).

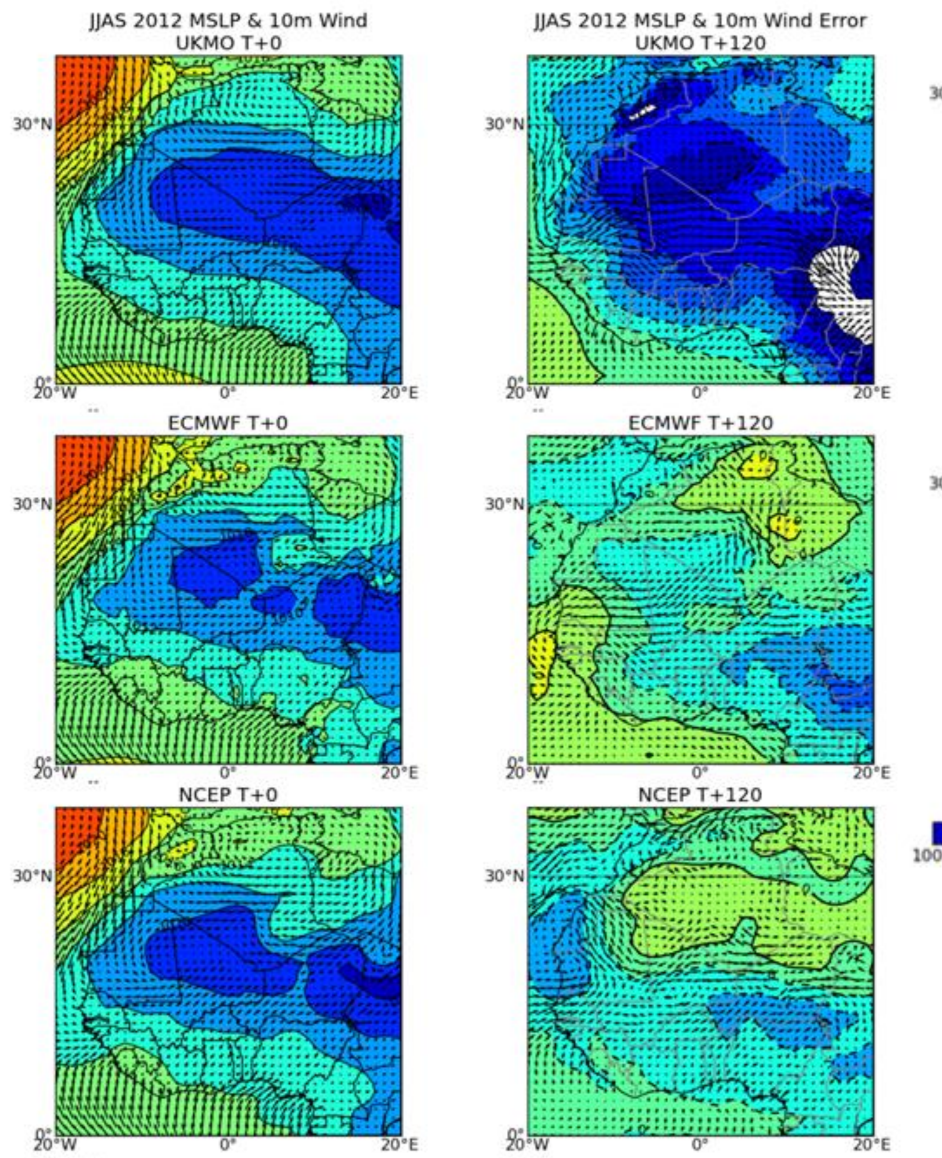

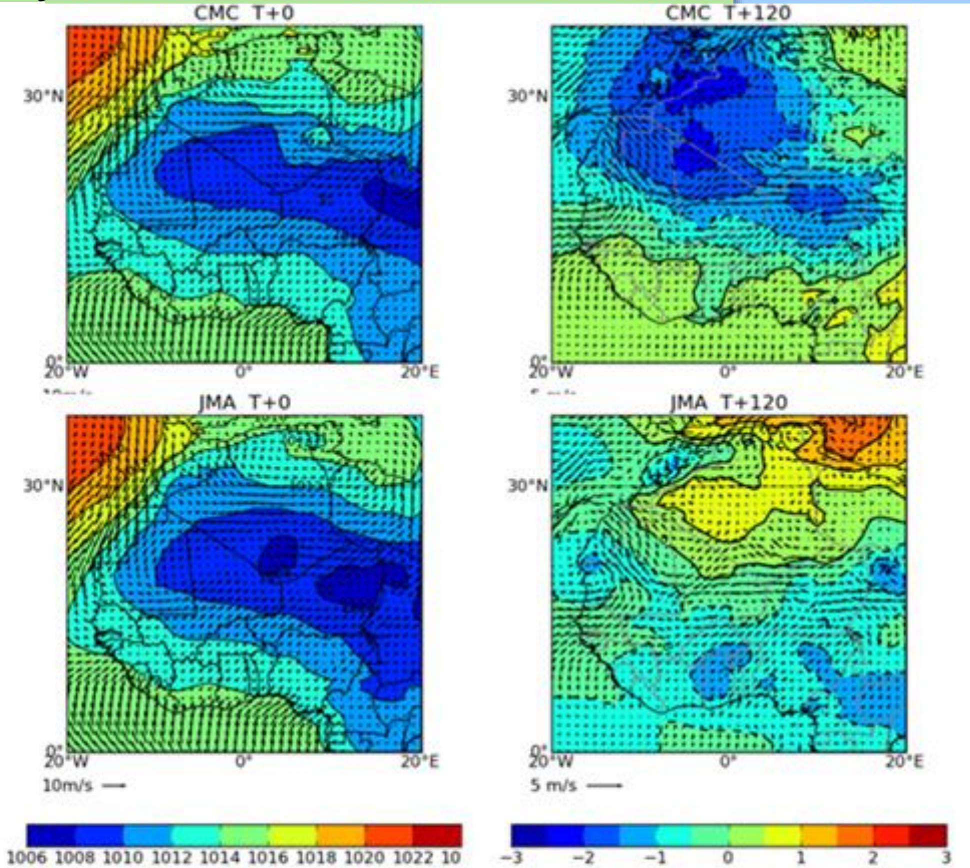

Figure 10.15: Low level monsoon flow (10 m wind vectors) and Saharan heat low (MSLP) for TIGGE analyses (left) and control forecast errors at T+120 (right).

Chapter 10: *Numerical Weather Prediction over Africa* – Lead author: Sean Milton

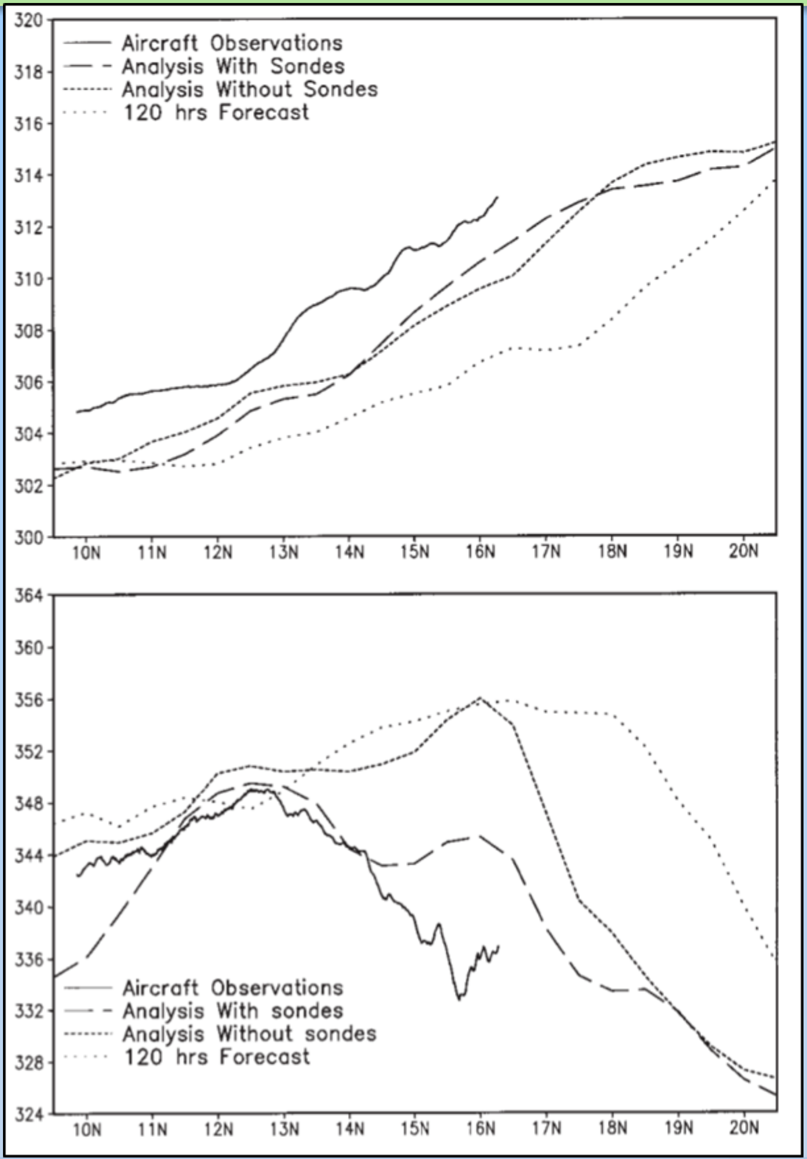

Figure 10.16: Meridional profiles of (top) potential temperature θ and (bottom) equivalent potential temperature θe based on aircraft observations on 28 August at a height of approximately 875 hPa (solid), between 1317 and 1538 UTC, ECMWF analysis for 1200 UTC 28 August with the dropsondes (long dashed), ECMWF analysis for 1200 UTC 28 August without dropsondes (small dashed), and the 5-day forecast from ECMWF for 1200 UTC 28 August (dotted). (reproduced from Fig. 7 of Thorncroft et al., 2003

African Monsoon Multidisciplinary Analysis

ACMAD

WMO

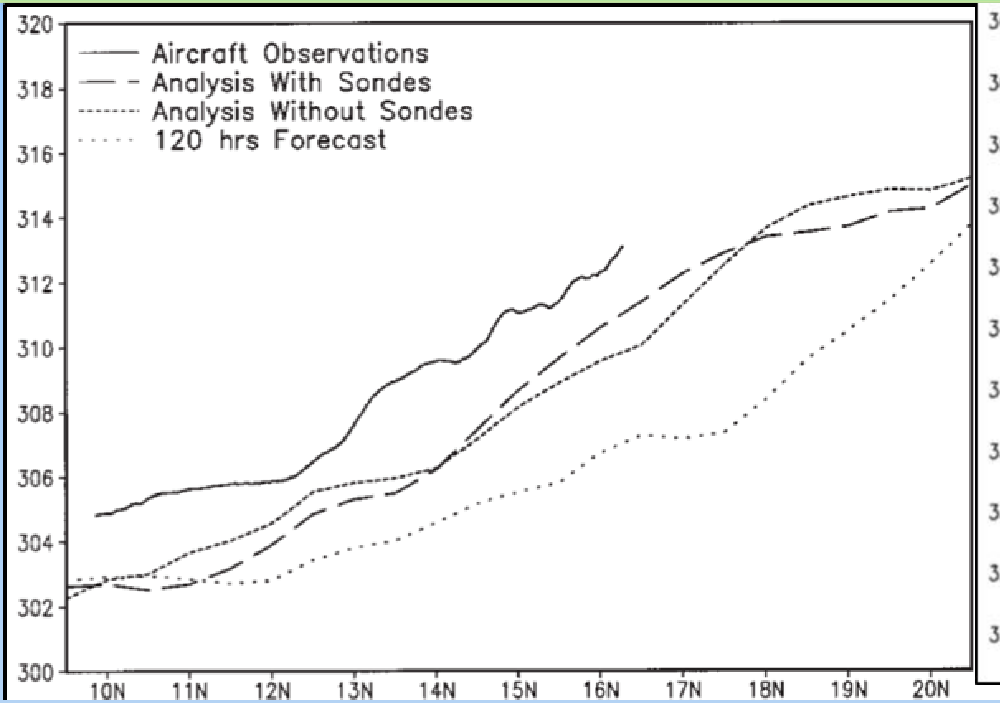

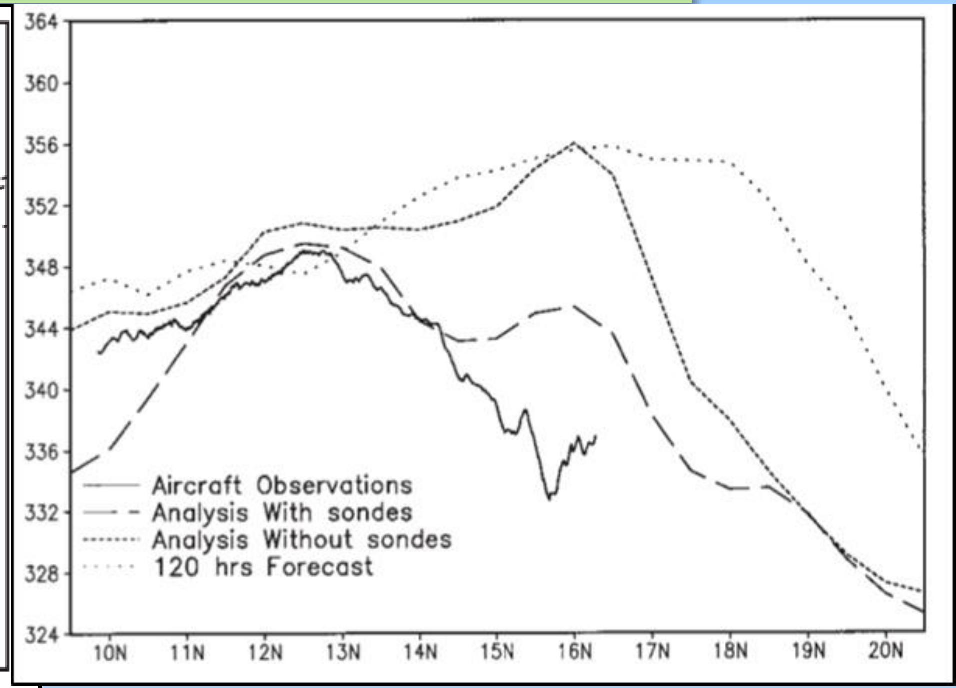

Figure 10.16: Meridional profiles of (top) potential temperature θ and (bottom) equivalent potential temperature θe based on aircraft observations on 28 August at a height of approximately 875 hPa (solid), between 1317 and 1538 UTC, ECMWF analysis for 1200 UTC 28 August with the dropsondes (long dashed), ECMWF analysis for 1200 UTC 28 August without dropsondes (small dashed), and the 5-day forecast from ECMWF for 1200 UTC 28 August (dotted). (reproduced from Fig. 7 of Thorncroft et al., 2003

ad author: Sean Milton

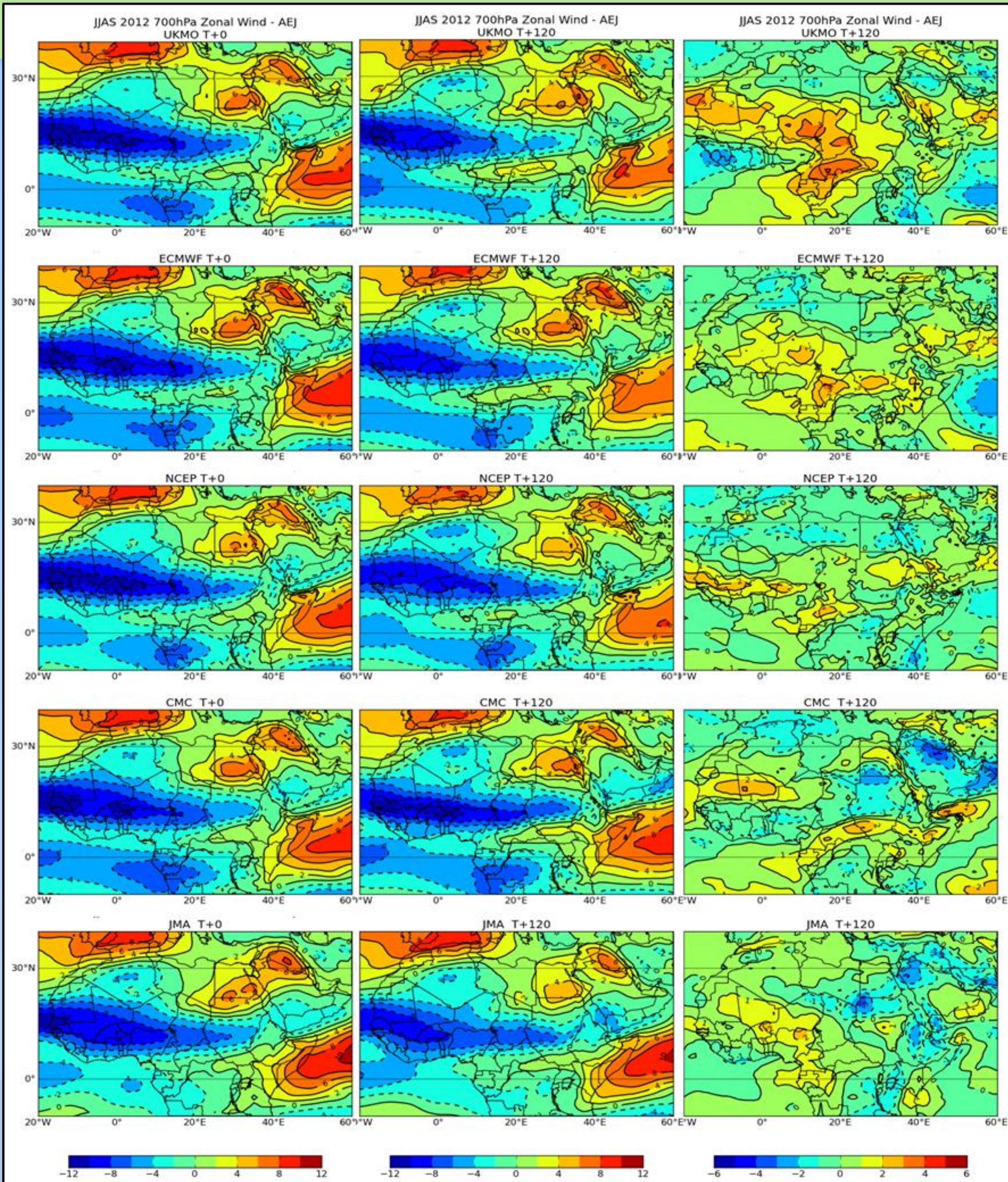

Figure 10.17: African Easterly Jet (AEJ) in TIGGE analyses (left) and T+120 forecasts (middle) shown by 700 hPa zonal winds. The T+120 mean errors in the AEJ are also shown (right)

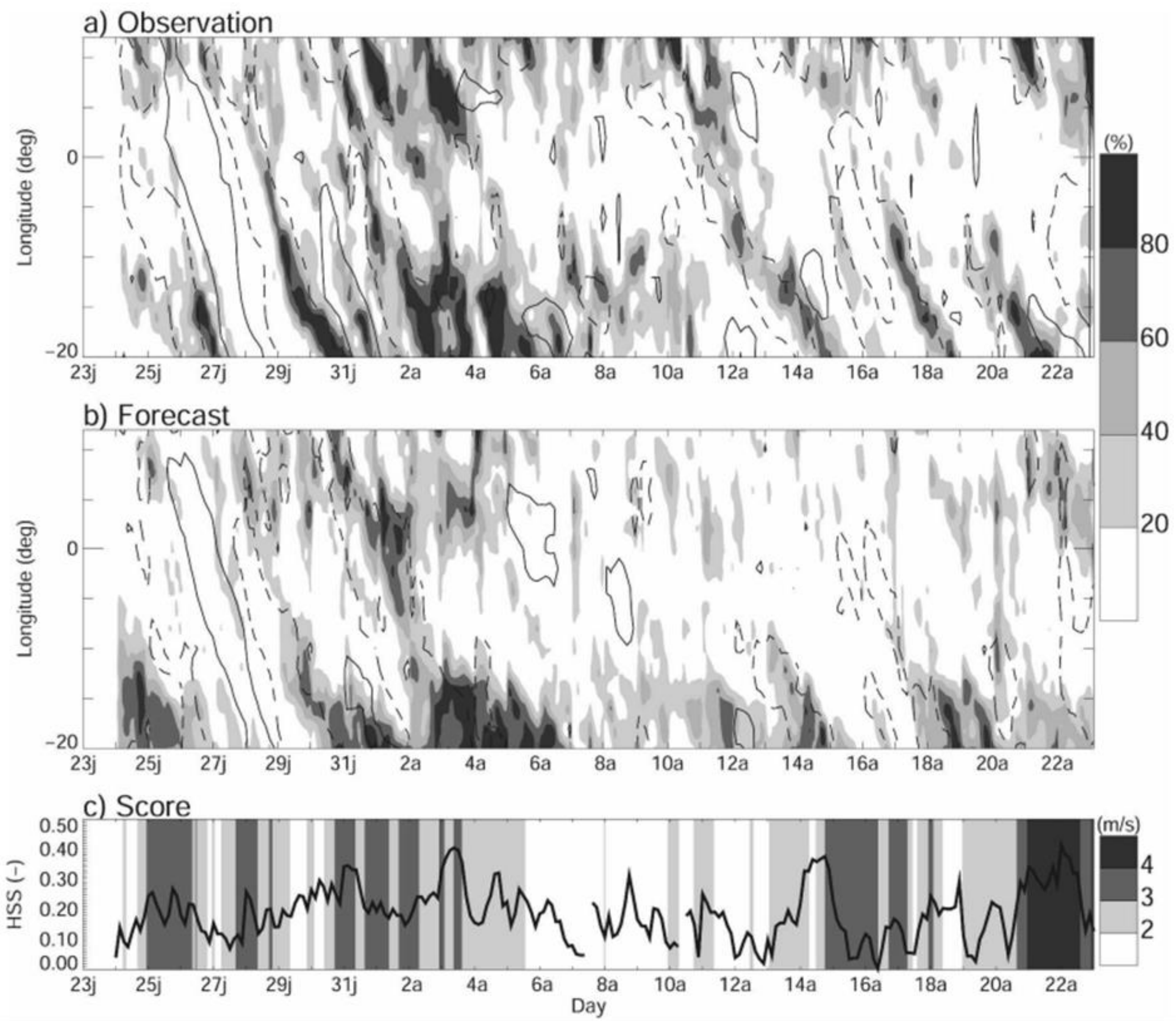

Figure 10.18 (a), (b): Time-longitude diagram of wind and cloud fraction averaged between 10° and 15°N from 23 July to 22 August 2006: MSG cloud fraction (shading, %) and 700-hPa meridional wind contours at -3 m/s (dashed) and at 3 m/s (solid). Fields are taken from (a) MSG observations and ECMWF analyses and (b) Méso-NH forecasts at D+1. (c) The time evolution of the HSS calculated point-by-point (line) and absolute meridional wind intensity from the analyses (shading, m/s) averaged over 10°–15°N. (reproduced from Fig. 7 of Sohne et al.(2008)

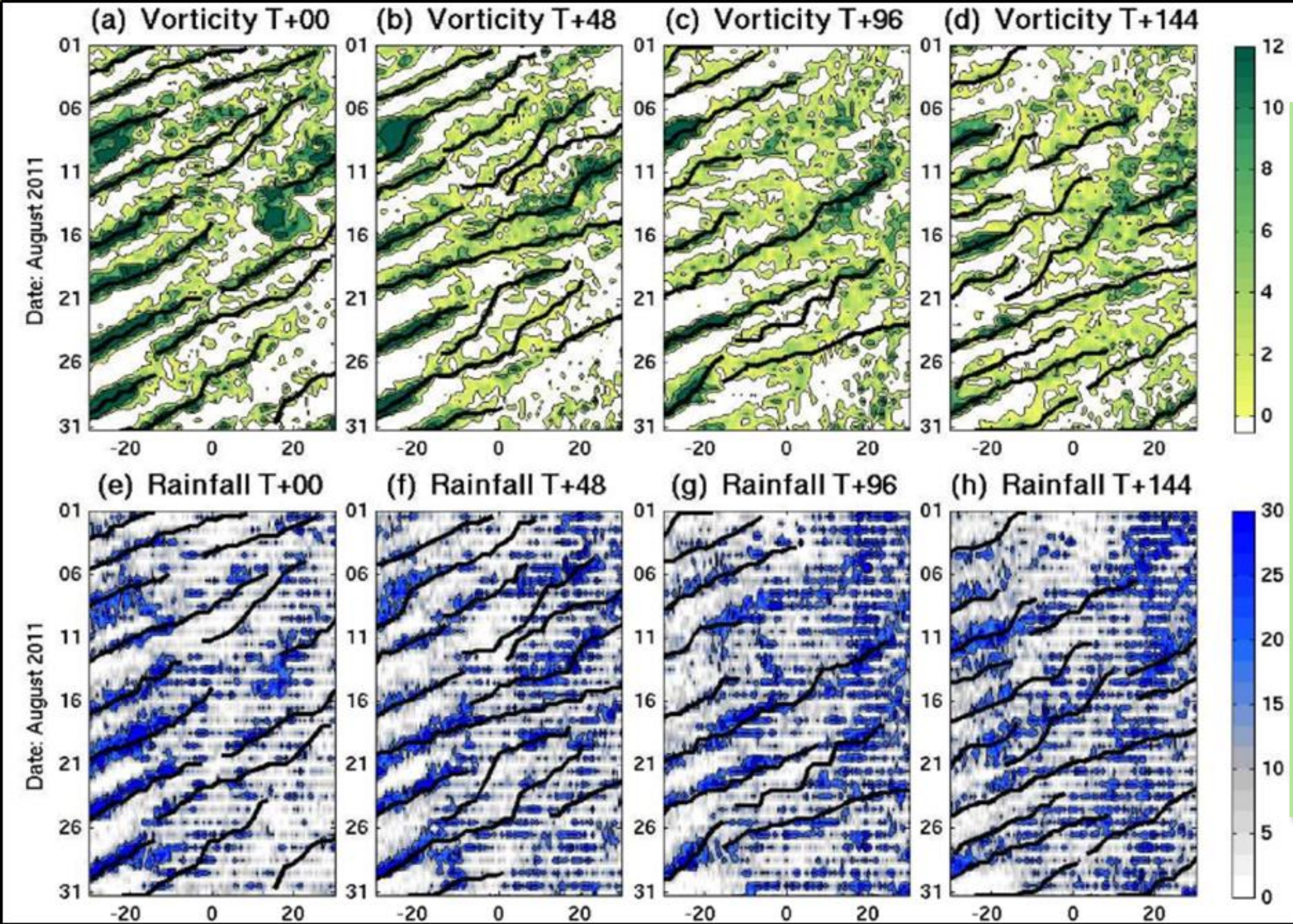

Figure 10.19: Example of NWP capability in Met Office operational deterministic global fore-casts from August 2011. The top panels show curvature vorticity and the bottom precipitation from the analysis and forecasts. The solid black lines are the tracks of the African Easterly Waves (AEW) using the objective tracking algorithm discussed in Bain et al. (2013).

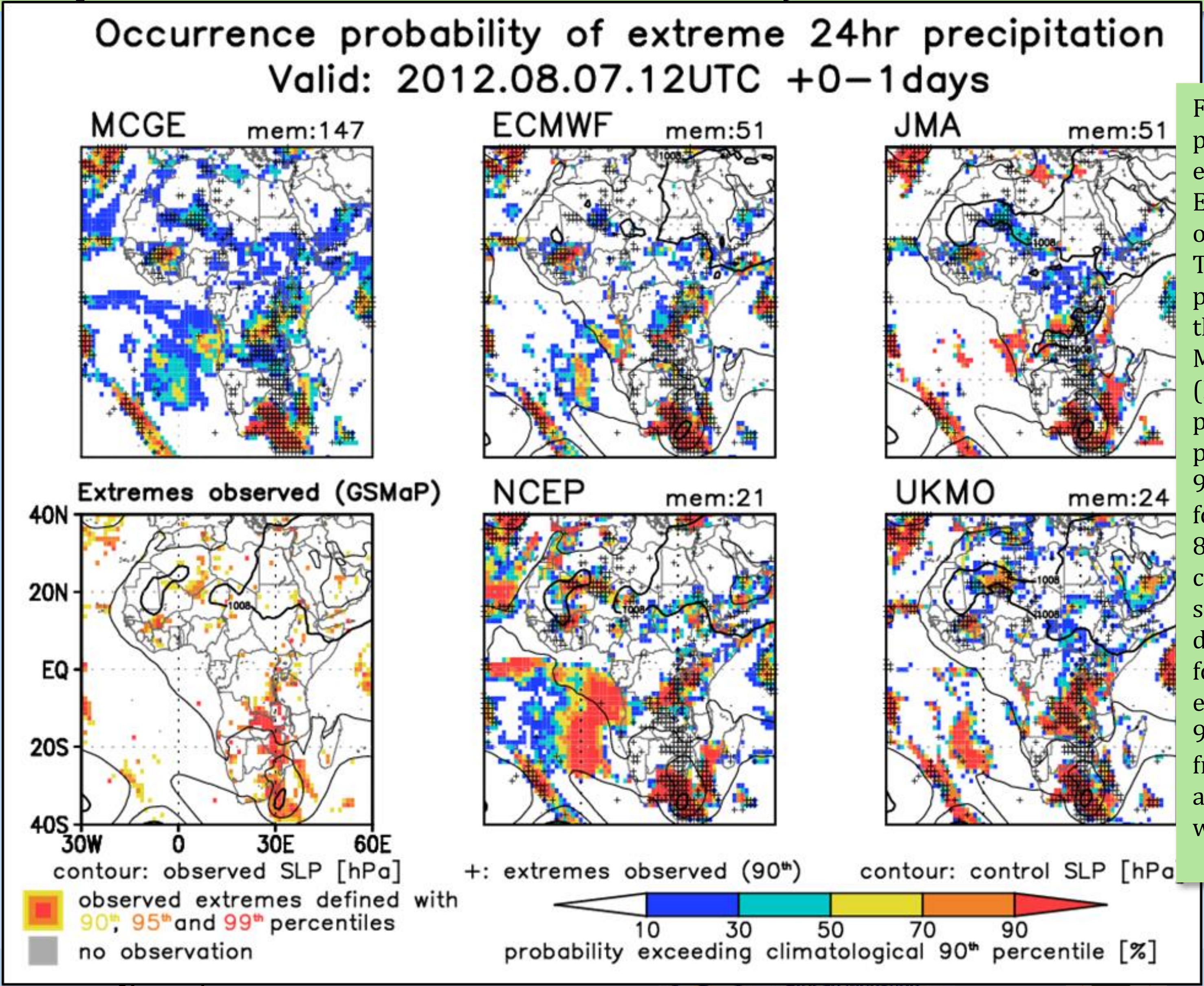

Figure 10.20: Ensemble based prediction of the risk of extreme precipitation. Example from TIGGE website of ensemble based predictions. This shows the ensemble prediction probabilities from the TIGGE models and the Multi Centre Grand Ensemble (MCGE) at 0-1 days for prediction of extreme precipitation (exceeding the 90th percentile). This is for the forecasts valid at 1200 UTC 7-8 August 2012, and corresponds to the case study shown in Figure 10.12 for the deterministic control forecasts. The observed extremes at 90th, 95th and 99th percentiles are shown from the GSMaP. These are also overlaid on each forecast with '+'.

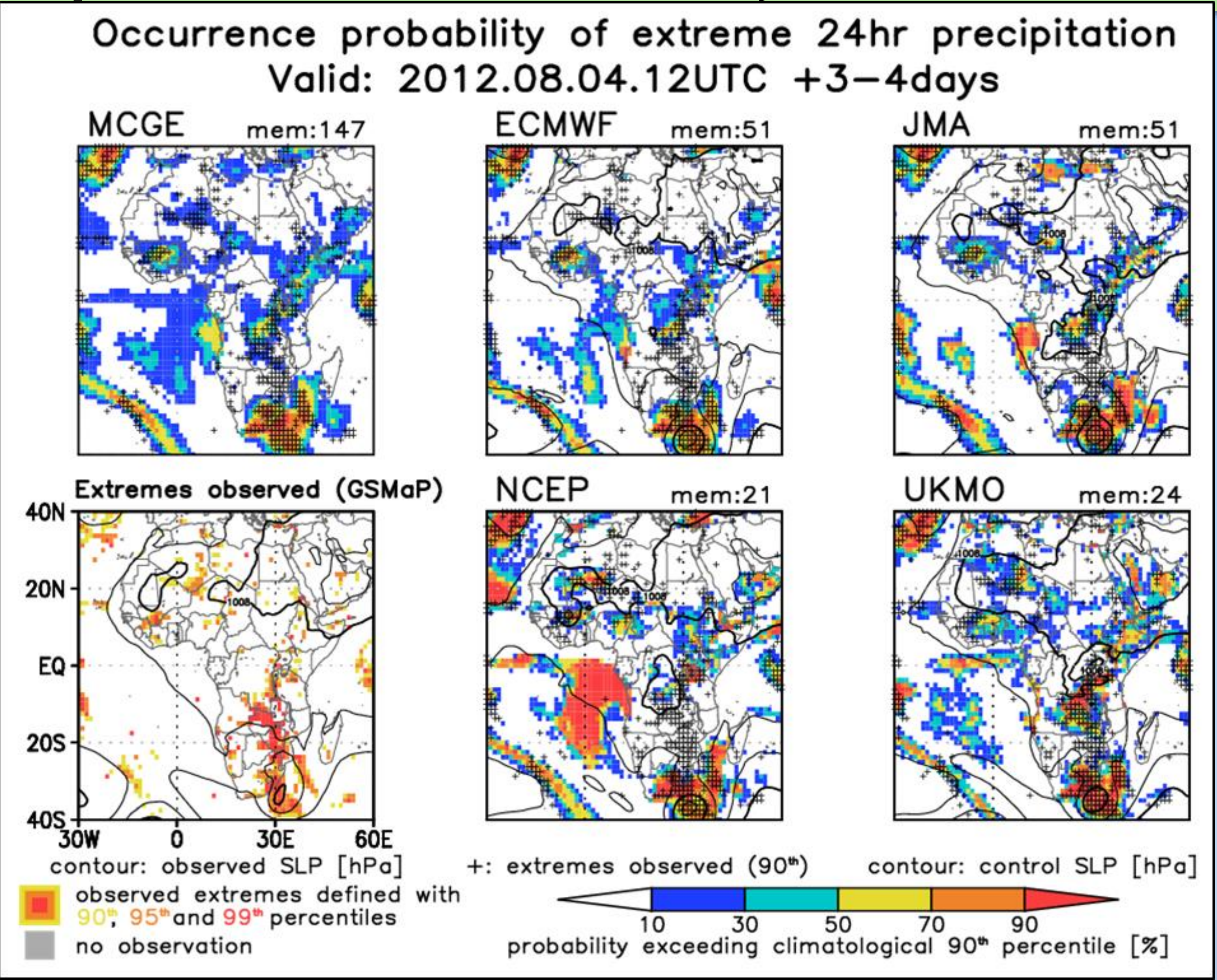

Figure 10.21: As Figure 10.20 but for days 3-4 forecasts valid at 1200 UTC 7th August 2012 and initialised on the 4th August at 1200 UTC.

ACMAD

WMO

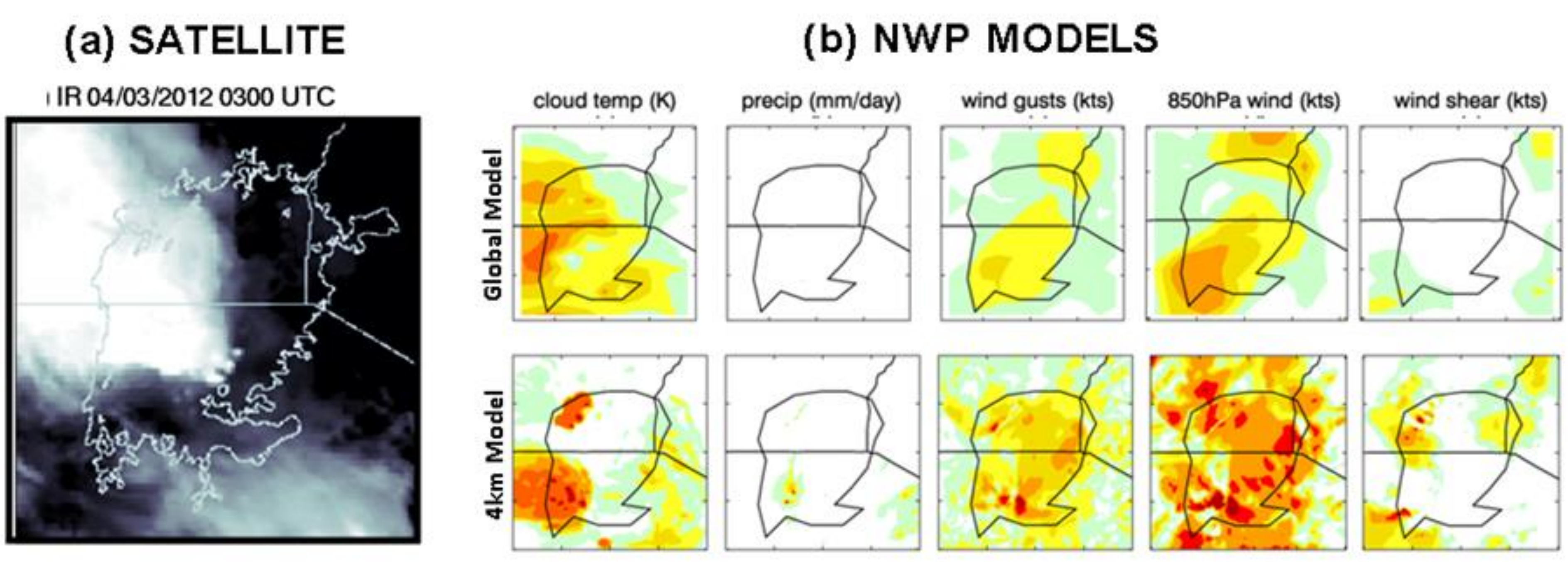

Figure 10.22: Case Study of Lake Victoria storm from 4th March 2012: (a) Satellite IR imagery (b) Met Office NWP operational model performance for Global and 4 km models. (Reproduced from Fig. 7, 8 and 9 of Chamberlain et al. (2013)